Complement-activated interferon-γ–primed human endothelium transpresents interleukin-15 to CD8+ T cells

Catherine B. Xie,[1] Bo Jiang,[2,3] Lingfeng Qin,[2] George Tellides,[2] Nancy C. Kirkiles-Smith,[1] Dan Jane-wit,[4] and Jordan S. Pober[1]

[1]Department of Immunobiology and [2]Department of Surgery, Yale University School of Medicine, New Haven, Connecticut, USA. [3]Department of Vascular Surgery, First Hospital of China Medical University, Shenyang, China. [4]Section of Cardiovascular Medicine, Department of Internal Medicine, Yale University School of Medicine, New Haven, Connecticut, USA.

Alloantibodies in presensitized transplant candidates deposit complement membrane attack complexes (MACs) on graft endothelial cells (ECs), increasing risk of CD8+ T cell–mediated acute rejection. We recently showed that human ECs endocytose MACs into Rab5+ endosomes, creating a signaling platform that stabilizes NF-κB–inducing kinase (NIK) protein. Endosomal NIK activates both noncanonical NF-κB signaling to synthesize pro–IL-1β and an NLRP3 inflammasome to process and secrete active IL-1β. IL-1β activates ECs, increasing recruitment and activation of alloreactive effector memory CD4+ T (Tem) cells. Here, we report that IFN-γ priming induced nuclear expression of IL-15/IL-15Rα complexes in cultured human ECs and that MAC-induced IL-1β stimulated translocation of IL-15/IL-15Rα complexes to the EC surface in a canonical NF-κB–dependent process in which IL-15/IL-15Rα transpresentation increased activation and maturation of alloreactive CD8+ Tem cells. Blocking NLRP3 inflammasome assembly, IL-1 receptor, or IL-15 on ECs inhibited the augmented CD8+ Tem cell responses, indicating that this pathway is not redundant. Adoptively transferred alloantibody and mouse complement deposition induced IL-15/IL-15Rα expression by human ECs lining human coronary artery grafts in immunodeficient mice, and enhanced intimal CD8+ T cell infiltration, which was markedly reduced by inflammasome inhibition, linking alloantibody to acute rejection. Inhibiting MAC signaling may similarly limit other complement-mediated pathologies.

Introduction

Human endothelial cells (ECs) perform immunosurveillance functions. Through basal expression of class I and class II MHC molecules and a subset of costimulatory molecules, human ECs can present antigens from local infections to circulating effector memory T cells (Tem cells) but not naive T cells, initiating recall responses (1). ECs lining vessels of solid organ allografts are perceived by the immune system as being infected and recognition of nonself class I MHC molecules complexed with a large number of different peptides displayed on graft ECs by circulating host CD8+ Tem cells triggers transendothelial migration, activation, and differentiation into cytotoxic T lymphocytes (CTLs) that mediate acute cell-mediated rejection (2, 3). In mice, circulating CD8+ T cell recognition of alloantigen in the vessel lumen, which is displayed on ECs, is sufficient and necessary to initiate rejection in the absence of alloantigen presentation by passenger dendritic cells (4). In humans, graft ECs also express class II MHC and the development of CD8+ Tem cells into CTLs is aided by activated CD4+ Tem cells that release IL-2 (5). Recent experiments with human immune system mice have revealed that ablation of class II MHC on ECs reduces T cell–mediated rejection, whereas ablation of class I MHC molecules eliminates it (5, 6).

Preformed complement fixing donor-specific antibodies in sensitized transplant candidates, assessed as panel reactive antibodies (PRAs), primarily react with nonself class I and class II MHC molecules on graft ECs and are a risk factor for acute and chronic rejection (7–9). PRAs binding to graft ECs activate complement and deposit complement membrane attack complexes (MACs), resulting in EC activation that increases the capacity of ECs to activate alloreactive CD4+ Tem cells (10, 11). Mechanistically, MACs are internalized through a clathrin-mediated process and delivered to Rab5+ endosomes. Endosomes containing internalized MACs recruit and stabilize NF-κB–inducing kinase (NIK), preventing its TRAF3-mediated polyubiquitinylation and rapid proteosomal degradation. Endosomal NIK activates 2 distinct responses: noncanonical NF-κB signaling to synthesize pro–IL-1β and assembly of an NLRP3 inflammasome that processes and secretes mature IL-1β (12). IFN-γ primes ECs to assemble NLRP3 inflammasomes and secrete IL-1 in response to MACs by increasing NLRP3, pro–caspase 1, and gasdermin D expression (12). IL-1β feeds back on the ECs to induce proinflammatory genes through a canonical NF-κB pathway that increases the capacity of the ECs to activate alloreactive CD4+ Tem cells. It has not been previously examined if PRAs can also increase the capacity of human ECs to activate CD8+ Tem cells, the effector cells responsible for acute rejection, through this or other pathways.

Interleukin-15 (IL-15) is pivotal in supporting the expansion and cytotoxicity of CD8+ memory T cells (13–15). IL-15 mediates its biological activity when displayed on a cell surface in complex with membrane-bound IL-15 receptor subunit alpha (IL-15Rα), which can be expressed by a variety of hematopoietic

Conflict of interest: The authors have declared that no conflict of interest exists.

Submitted: November 19, 2019; **Accepted:** March 11, 2020; **Published:** May 26, 2020.
Reference information: *J Clin Invest*. 2020;130(7):3437–3452.
https://doi.org/10.1172/JCI135060.

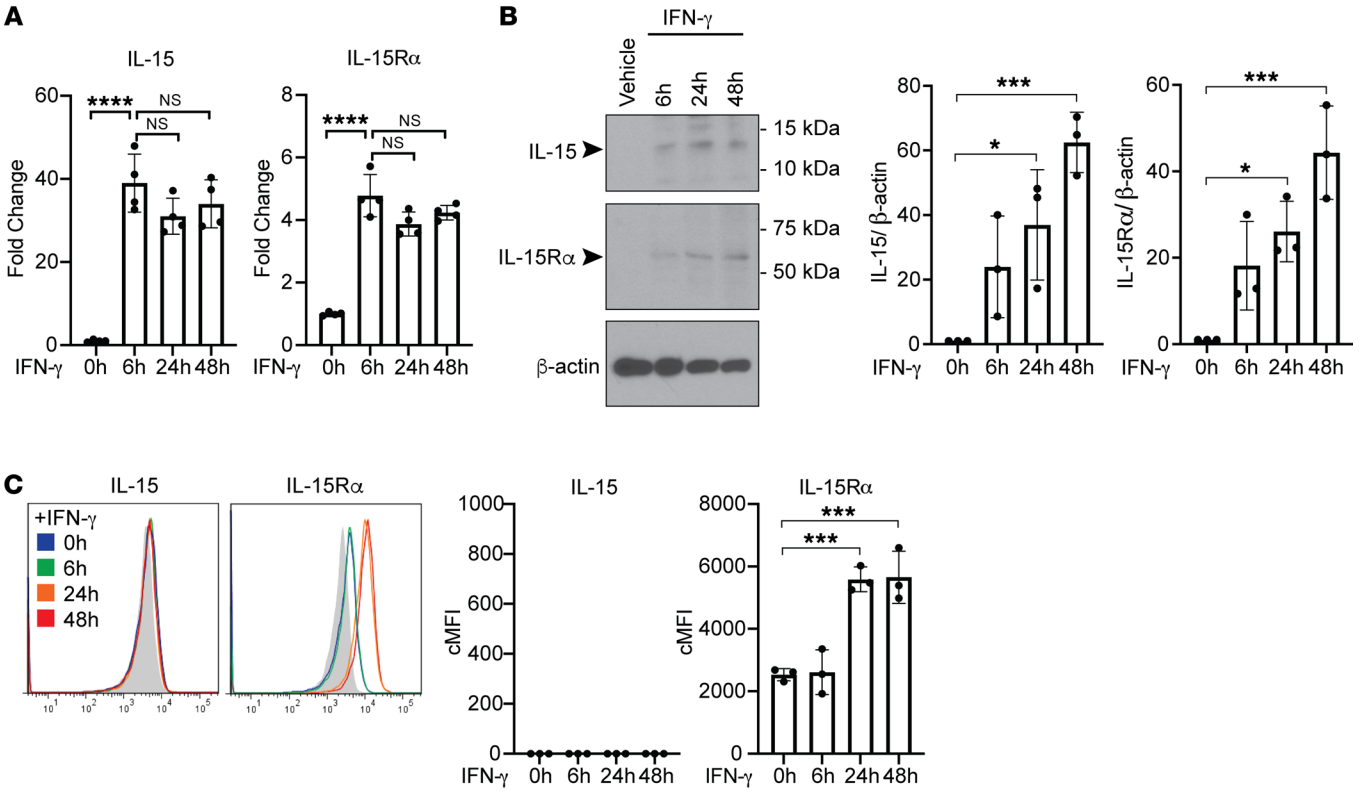

Figure 1. IFN-γ induces human ECs to upregulate expression of intracellular IL-15 and IL-15Rα and surface IL-15Rα. (**A**) ECs were treated with IFN-γ for 6 hours, 24 hours, and 48 hours. IL-15 and IL-15Rα transcript levels were assessed by qRT-PCR ($n = 4$). (**B**) After IFN-γ treatment for 6 hours, 24 hours, and 48 hours, EC cell lysates were analyzed for IL-15 and IL-15Rα by immunoblotting. Densitometric values of IL-15 and IL-15Rα bands on exposed immunoblots from 3 independent experiments using 3 HUVEC donors were calculated and normalized to the intensity of β-actin bands ($n = 3$). (**C**) ECs were treated with IFN-γ for 6 hours, 24 hours, and 48 hours and analyzed for surface IL-15 and IL-15Rα staining by flow cytometry. FACS plots show a representative experiment ($n = 3$). Data represent mean SEM. $^*P < 0.05$; $^{***}P < 0.001$; $^{****}P < 0.0001$; 1-way ANOVA and Tukey's multiple comparisons test. Representative of 3 independent experiments using 3 HUVEC donors.

and parenchymal cell types (14, 16, 17). The surface-expressed IL-15/IL-15Rα complex may then be presented in *trans* to $CD8^+$ memory T cells expressing an IL-2Rβ and common γ chain (γ_c); the same process can also activate natural killer (NK) cells (18, 19). IL-15 thus functions in the context of cell-cell contact and can deliver signals together with costimulatory molecules as part of an immunological synapse (20, 21). While IL-15 mRNA is more widely produced, IL-15 protein expression is tightly controlled and very little IL-15 is secreted (22). Furthermore, the IL-15/IL-15Rα complex binds to IL-2βγ$_c$ with much higher affinity than does free IL-15 (16, 23). Interestingly, nonsecretable IL-15 has been reported to be stored intracellularly, appearing in the nucleus and cytoplasmic components, suggesting some intracrine biological functions for IL-15 (24, 25). While IL-15 production has been largely studied on monocytes and DCs, ECs stimulated with IFN-γ have been reported to have enhanced ability compared with unstimulated ECs to bind added recombinant IL-15 in vitro, consistent with induction of IL-15Rα (26). In addition, a recent study found that IL-1β administration conditioned host murine cells, in particular through actions on vascular ECs, to induce granzyme B induction of adoptively transferred T cells, which led to a greater antitumor response that was dependent on IL-2 and IL-15 (27). While the source of IL-15Rα in this study was suggested to be splenic neutrophils, the data are consistent with the possibility that IL-1β directly induces IL-15/IL-15Rα expression on ECs.

Here, we report that IFN-γ induces nuclear but not surface expression of both IL-15 and IL-15Rα in human ECs and that in response to antibody-mediated complement activation, the endosomal MAC/NLRP3 inflammasome/IL-1β signaling pathway in IFN-γ–primed ECs induces translocation of IL-15/IL-15Rα to the cell surface, enabling IL-15/IL-15Rα transpresentation by ECs to $CD8^+$ Tem cells. This pathway both intensifies allogeneic Tem cell responses to human ECs in culture and T cell–mediated rejection of human artery grafts in human immune system mice.

Results

IFN-γ induces human ECs to upregulate intracellular IL-15 and IL-15Rα expression and unbound surface IL-15Rα. Both class I and II MHC molecules, the targets of pretransplant panel reactive antibodies (PRAs), are highly expressed by human ECs in situ, but, in the absence of IFN-γ, are downregulated in cell culture (28). Therefore, to model in vivo effects of human alloantibodies on human ECs, we routinely reinduce MHC expression on cultured ECs by IFN-γ treatment. Our previous studies revealed that IFN-γ markedly enhances the proinflammatory effects of PRA-mediated

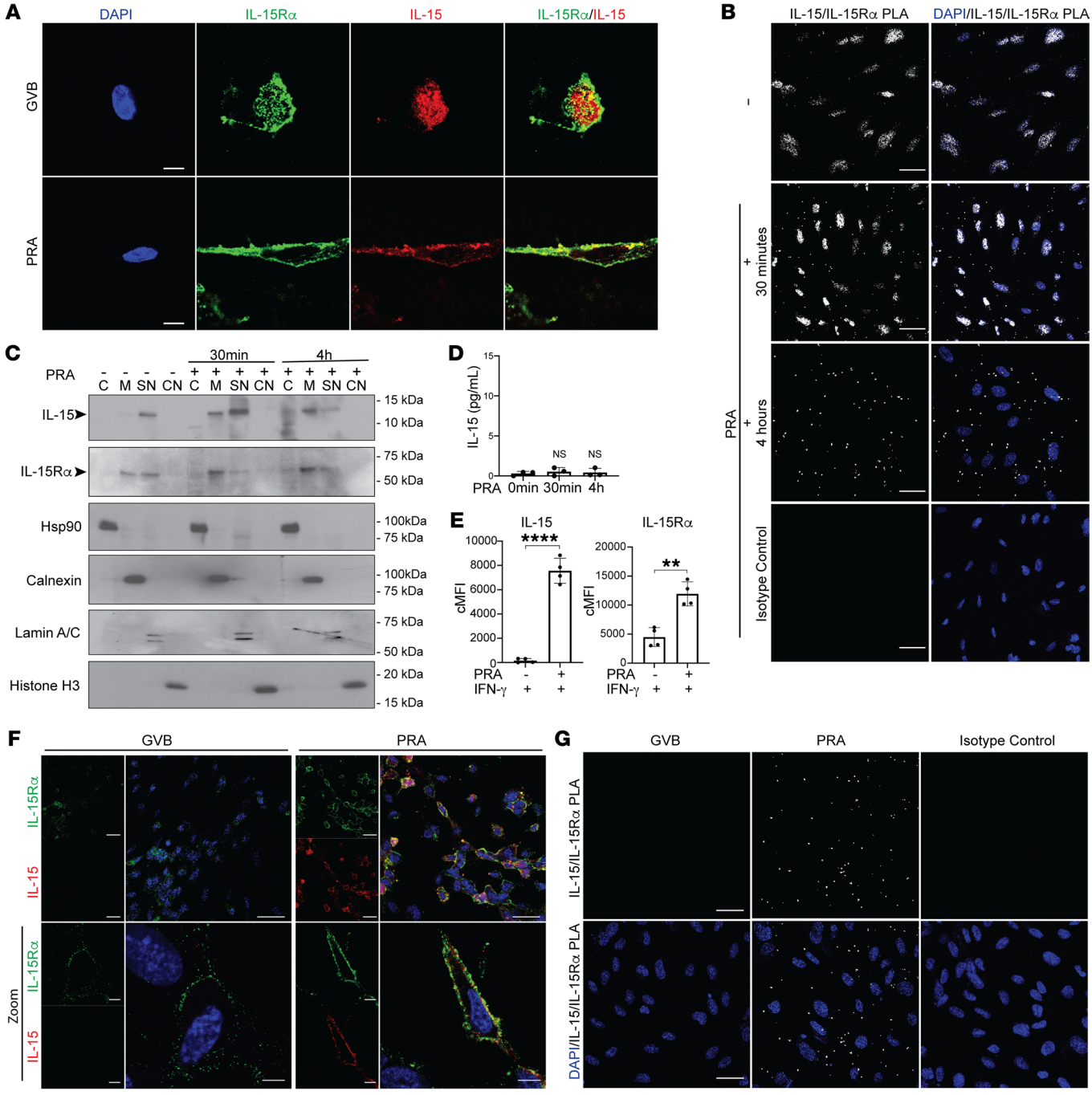

Figure 2. MAC induces nuclear translocation and coordinate expression of IL-15/IL-15Rα on the cell surfaces of IFN-γ-primed human ECs. (**A**) Representative images of confocal microcopy analysis of ECs that were pretreated with IFN-γ for 48 hours before being treated with PRA for 30 minutes or 4 hours, fixed and permeabilized, and stained for intracellular IL-15 and IL-15Rα. Scale bars: 5 μm. (**B**) IFN-γ–pretreated ECs were treated with either gelatin veronal buffer (GVB) control or PRA sera treatment, fixed and permeabilized prior performing PLA between IL-15 and IL-15Rα. Representative images of confocal microscopy analysis. Scale bars: 30 μm. (**C**) IFN-γ–pretreated ECs were treated with either GVB or PRA for 30 minutes and 4 hours. Extracts from 4 specific cellular compartments (cytoplasmic [C], membrane [M], soluble nuclear [SN], and chromatin-bound nuclear [CN]) were isolated by stepwise lysis and analyzed for IL-15 and IL-15Rα protein by immunoblotting. (**D**) ELISA measurements of IL-15 in culture supernatants of IFN-γ–primed ECs treated with PRA sera. (**E**) ECs were pretreated with IFN-γ for 48 hours before PRA treatment and analysis of surface staining IL-15 and IL-15Rα by flow cytometry (n = 4). (**F**) Representative images of confocal immunofluorescence analysis of IL-15 and IL-15Rα surface staining on unpermeabilized IFN-γ–pretreated ECs treated with either PRA sera or control GVB. Scale bars for top row: 30 μm; scale bars for "Zoom" bottom row: 5 μm. (**G**) IFN-γ–pretreated ECs were treated with either GVB control or PRA sera treatment. Proximity ligation assay (PLA) was performed between surface IL-15 and IL-15Rα and analyzed by confocal microscopy. Scale bars: 30 μm. Data represent mean ± SEM. *P < 0.05; **P < 0.01; ***P < 0.001; ****P < 0.0001; 1-way ANOVA and Tukey's multiple comparisons test in **D** and unpaired 2-tailed Student's t test in **E**. Representative of 3 independent experiments using 3 HUVEC donors.

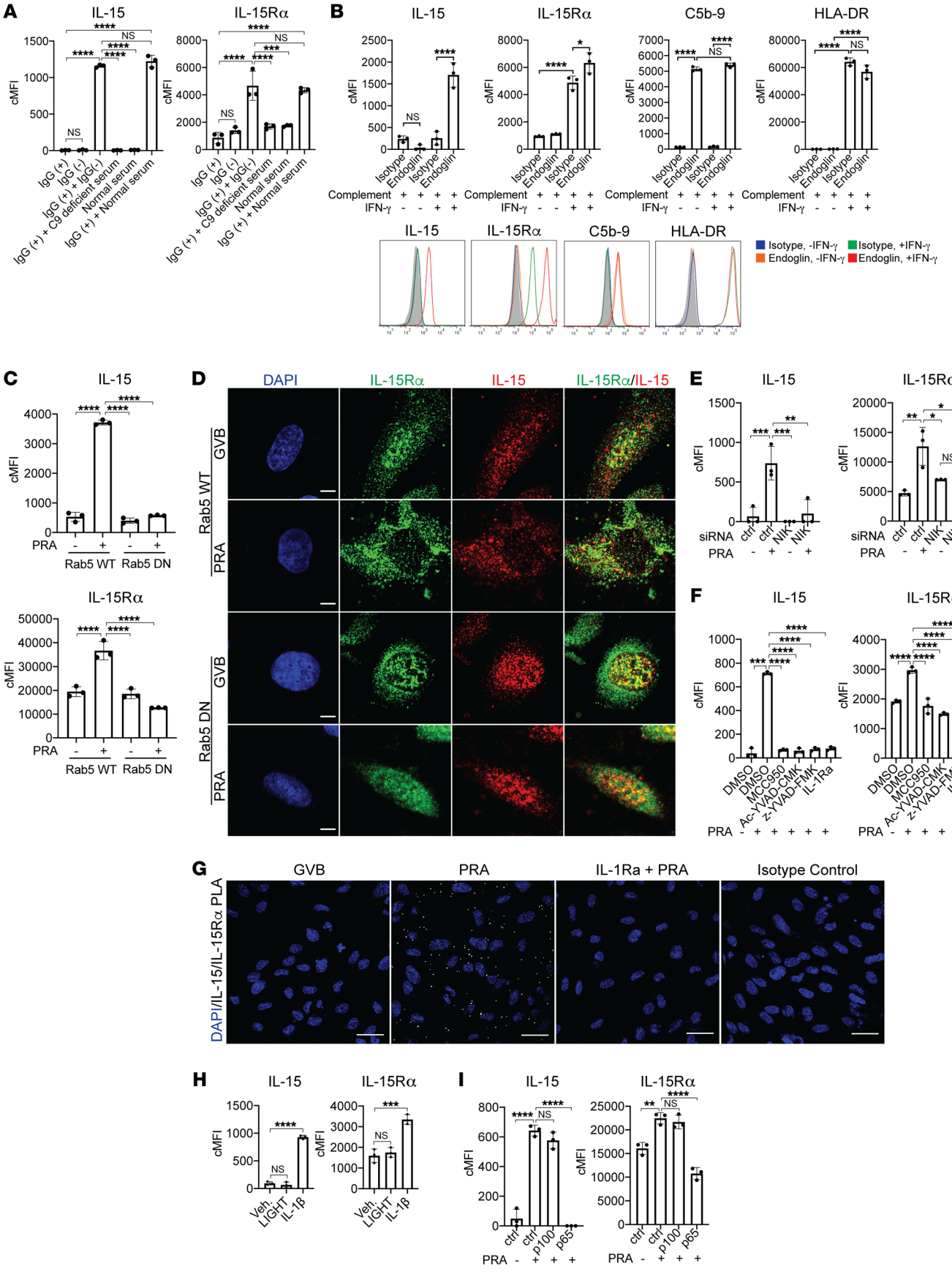
A
IL-15
IL-15Rα
cMFI
IgG (+)
IgG (-)
IgG (+) + IgG(-)
IgG (+) + C9 deficient serum
Normal serum
IgG (+) + Normal serum
B
IL-15
IL-15Rα
C5b-9
HLA-DR
Isotype
Endoglin
Complement
IFN-γ
Isotype, -IFN-γ
Isotype, +IFN-γ
Endoglin, -IFN-γ
Endoglin, +IFN-γ
C
IL-15
IL-15Rα
PRA
Rab5 WT
Rab5 DN
D
DAPI
IL-15Rα
IL-15
IL-15Rα/IL-15
Rab5 WT
Rab5 DN
GVB
PRA
E
IL-15
IL-15Rα
siRNA
ctrl
NIK
F
IL-15
IL-15Rα
DMSO
MCC950
Ac-YVAD-CMK
z-YVAD-FMK
IL-1Ra
G
GVB
PRA
IL-1Ra + PRA
Isotype Control
DAPI/IL-15/IL-15Rα PLA
H
IL-15
IL-15Rα
Veh.
LIGHT
IL-1β
I
IL-15
IL-15Rα
ctrl
p100
p65

Figure 3. MAC stabilization of endosomal NIK, activation of NLRP3 inflammasome, and IL-1 signaling drives nuclear translocation and induction of IL-15/IL-15Rα complexes on human EC cell surfaces. (**A**) PRA sera was separated into IgG^+ and IgG^- fractions and added to IFN-γ–pretreated ECs alone or in combination with C9-deficient or normal serum before flow cytometry analysis of surface IL-15 and IL-15Rα (n = 3). (**B**) Unprimed and IFN-γ–primed ECs were incubated with complement-fixing anti–human endoglin IgG_{2a} antibody and human complement before flow cytometry analysis of IL-15, IL-15Rα, HLA-DR, and C5b-9 (n = 3). (**C**) IFN-γ–primed and stably transduced Rab5-WT or Rab5-DN (S43N) ECs were treated with PRA sera or control GVB and stained for surface IL-15 and IL-15Rα (n = 3). (**D**) IFN-γ–primed Rab5-WT and Rab5-DN ECs were treated with PRA and stained for intracellular IL-15 and IL-15Rα. Scale bars: 5 μm. (**E**) IFN-γ–pretreated ECs were transfected with NIK siRNA, treated with PRA, and analyzed for surface IL-15 and IL-15Rα (n = 3). (**F**) IFN-γ–primed ECs were pretreated with NLRP3 inhibitor MCC950, caspase-1 inhibitors Ac-YVAD-CMK or z-YVAD-FMK, or IL-1 receptor antagonist (IL-1Ra), treated with PRA and analyzed for surface IL-15 and IL-15Rα (n = 3). (**G**) IFN-γ–primed ECs were pretreated with either vehicle or IL-1Ra before PRA treatment. Proximity ligation assay (PLA) was performed between surface IL-15 and IL-15Rα and analyzed by confocal microscopy. Scale bars: 30 μm. (**H**) IFN-γ–primed ECs were treated with LIGHT, IL-1β, or mock treatment before analysis of surface IL-15 and IL-15Rα (n = 3). (**I**) IFN-γ–primed ECs were transfected with control, p100, or p65 siRNA before PRA treatment and flow cytometry analysis for surface IL-15 and IL-15Rα (n = 3). Data represent mean ± SEM. $^{**}P < 0.01$; $^{****}P < 0.0001$; 1-way ANOVA and Tukey's multiple comparisons test. Representative of 3 independent experiments using 3 HUVEC donors.

complement activation and MAC signaling on human ECs, as would be expected with increased antibody binding (12). However, the actions of IFN-γ not only increased expression of MHC molecules, our rationale for using this pretreatment, but also induced expression of NLRP3, pro–caspase-1, and gasdermin D, actions that prime human ECs for NLRP3 inflammasome formation. Consequently, priming with IFN-γ also increased MAC signaling when deposited by antibody that targeted a surface antigen not induced by IFN-γ. Since ECs in situ appear to be primed by IFN-γ as evidenced by basal MHC molecule expression, we began this study by examining the effects of IFN-γ on the intracellular and cell surface expression of both IL-15 and IL-15Rα in human ECs. To do so, we performed a time course of IFN-γ treatment of human ECs using a recombinant human IFN-γ concentration known to saturate receptors (50 ng/mL) and analyzed transcript and whole cell protein levels of IL-15 and IL-15Rα. We found that IFN-γ alone significantly increased transcript levels of IL-15 and IL-15Rα and cell-associated protein levels beginning at 6 hours and sustained through 48 hours, as detected by quantitative reverse transcription PCR (qRT-PCR) and immunoblotting, respectively (Figure 1, A and B). However, when we examined the surface expression of IL-15 and IL-15Rα on ECs with and without IFN-γ treatment by flow cytometry of unpermeabilized cells, we found that IFN-γ treatment upregulated the surface expression of IL-15Rα after 24 hours and 48 hours but that IL-15 surface expression was undetectable at all time points (Figure 1C). IL-15 and IL-15Rα staining of IFN-γ–treated ECs after permeabilization showed colocalization of both proteins in the nucleus but only IL-15Rα, and not IL-15, could also be found outside of the nucleus (Figure 2A, top row). To directly assess protein-protein association, proximity ligation assay (PLA) was conducted between IL-15 and IL-15Rα using 2 primary antibodies that were specific for either human IL-15 or IL-15Rα on permeabilized ECs. An IL-15/IL-15Rα PLA signal was detected in the nucleus of IFN-γ–pretreated ECs, indicating that IL-15 not only colocalizes but is associated with its receptor in the nucleus (Figure 2B, top row). PLA assay between IL-15Rα and histone H1, an irrelevant nuclear protein as a negative control, did not yield any detectable signal compared with the positive PLA signals detected between IL-15 and IL-15Rα, demonstrating the PLA signal specificity of the IL-15/IL-15Rα complex interaction (Supplemental Figure 1; supplemental material available online with this article; https://doi.org/10.1172/JCI135060DS1). These data indicate that IFN-γ induces formation of nuclear IL-15 and IL-15Rα complexes in human ECs and while some cell-surface IL-15Rα expression is induced in response to IFN-γ, it is not coordinately expressed with surface IL-15 under these treatment conditions.

Alloantibody and complement activation induce nuclear translocation and coordinate expression of IL-15/IL-15Rα complexes on the cell surfaces of IFN-γ–primed human ECs. We next examined the effects of PRA binding and MAC assembly on IL-15/IL-15Rα expression in IFN-γ–pretreated human ECs. Specifically, we examined the intracellular localization of IL-15 or IL-15Rα with and without PRA stimulation. By immunofluorescence microscopy and PLA assay between IL-15 and IL-15Rα, we observed that PRA treatment induced IL-15/IL-15Rα complexes to translocate from the nucleus to the cell periphery (Figure 2, A and B). We further examined the localization of IL-15 and IL-15Rα in IFN-γ–pretreated human ECs upon PRA stimulation by subcellular fractionation and immunoblotting. IL-15 and IL-15Rα protein were both detected in the soluble nuclear protein extract, with IL-15Rα also detectable in the membrane extract at baseline in IFN-γ–pretreated and vehicle-treated ECs. Upon PRA stimulation, decreased IL-15 and IL-15Rα were detected in the nuclear extract, with concurrent increased detection in the membrane bound extract. There was no detectable shift in the band size of either protein by immunoblotting (Figure 2C and Supplemental Figure 2). Culture supernatants collected from PRA-treated ECs did not contain detectable levels of IL-15 (Figure 2D). These observations suggested that PRA treatment could result in IL-15 and IL-15Rα being expressed on EC cell surfaces rather than being secreted. To test this directly, we used flow cytometry and confocal immunofluorescence microscopy of unpermeabilized cells. Both techniques confirmed that the disappearance of these molecules from the cytosol resulted in cell-surface expression (Figure 2, E and F), a prerequisite for transpresentation to lymphocytes. To more directly assess whether IL-15 was bound to IL-15Rα on the EC surfaces after PRA stimulation, we performed a PLA between IL-15 and IL-15Rα on unpermeabilized ECs in order to detect surface interactions. IL-15 and IL-15Rα protein interactions were detected only on the surfaces of PRA-treated and not on vehicle-treated ECs, indicating that the membrane-bound IL-15Rα of unstimulated and IFN-γ–pretreated ECs were unoccupied receptors and that PRA-induced surface IL-15 is associated with IL-15Rα on ECs (Figure 2G). Minimal signal was detected in the isotype controls, indicating low background and high specificity. These data collectively indicate that after IFN-γ upregulation of nuclear IL-15/IL-15Rα complexes and upon PRA and complement activation, IL-15/IL-15Rα complexes translocate from the nucleus to the cell surface where they are available for transpresentation.

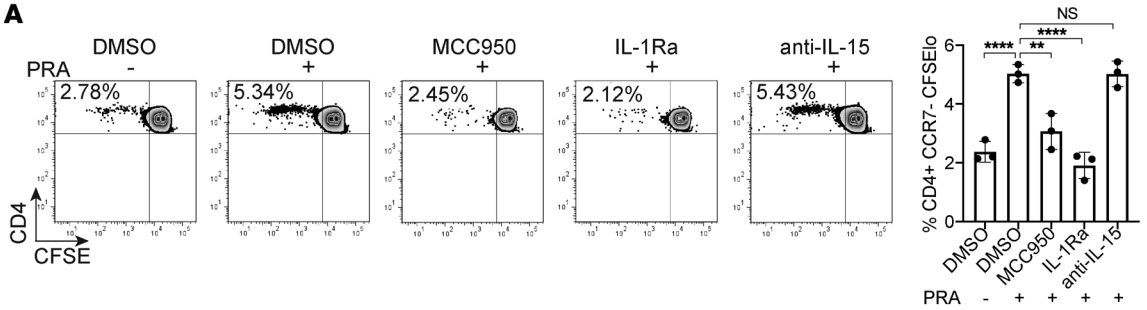
A
DMSO
DMSO
MCC950
IL-1Ra
anti-IL-15
PRA - + + + +
2.78%
5.34%
2.45%
2.12%
5.43%
CD4
CFSE
% CD4+ CCR7- CFSElo
NS
****
**

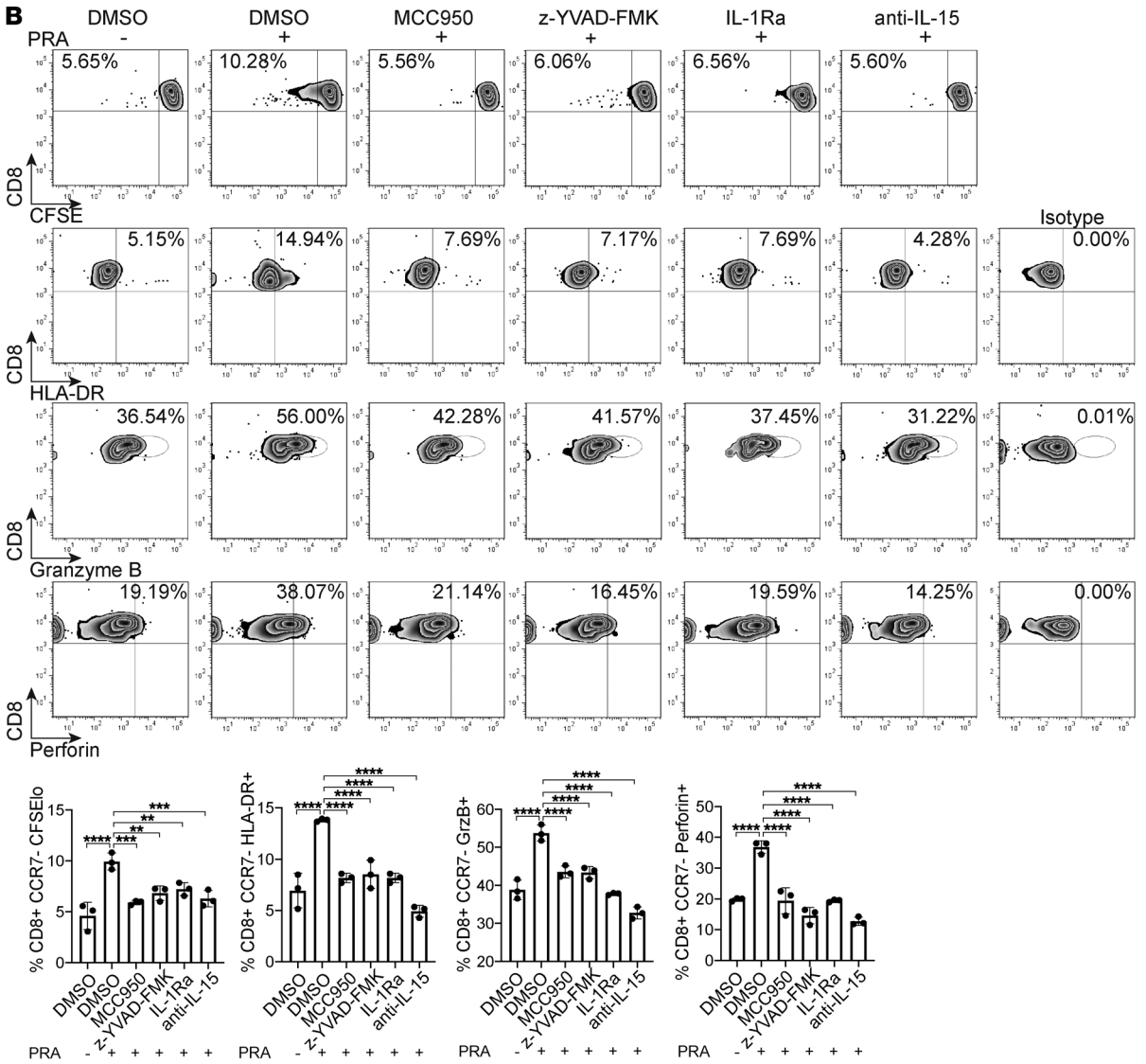
B
DMSO
DMSO
MCC950
z-YVAD-FMK
IL-1Ra
anti-IL-15
PRA - + + + + +
5.65%
10.28%
5.56%
6.06%
6.56%
5.60%
CD8
CFSE
Isotype
5.15%
14.94%
7.69%
7.17%
7.69%
4.28%
0.00%
HLA-DR
36.54%
56.00%
42.28%
41.57%
37.45%
31.22%
0.01%
Granzyme B
19.19%
38.07%
21.14%
16.45%
19.59%
14.25%
0.00%
Perforin
% CD8+ CCR7- CFSElo
% CD8+ CCR7- HLA-DR+
% CD8+ CCR7- GrzB+
% CD8+ CCR7- Perforin+

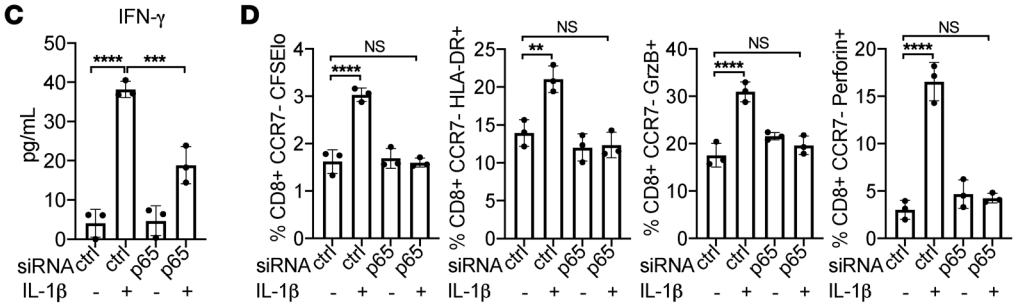
C
IFN-γ
pg/mL
siRNA ctrl ctrl p65 p65
IL-1β - + - +
D
% CD8+ CCR7- CFSElo
% CD8+ CCR7- HLA-DR+
% CD8+ CCR7- GrzB+
% CD8+ CCR7- Perforin+
NS

Figure 4. Surface IL-15 on MAC-activated ECs is presented in *trans* and enhances allogeneic CD8⁺ Tem cell activation, proliferation, and differentiation. (**A**) Proliferation of CD4⁺ Tem cells after coculture for 7 days with IFN-γ–primed ECs pretreated with NLRP3 inflammasome inhibitor MCC950, IL-1 receptor antagonist, anti–IL-15 blocking antibody, or DMSO before PRA sera or vehicle treatment for 6 hours. CFSE dilution was assessed on day 7 by flow cytometry. FACS plots show a representative experiment (n = 3). (**B**) CD8⁺ Tem cell proliferation by CFSE dilution, activation by HLA-DR surface expression, and differentiation by granzyme B and perforin expression were assessed after coculture with IFN-γ–primed ECs pretreated with MCC950, z-YVAD-FMK, IL-1Ra, anti–IL-15 blocking antibody, or DMSO before PRA sera or vehicle treatment for 6 hours. Flow cytometry analysis was performed after 7 days of coculture. FACS plots show a representative experiment (n = 3). (**C**) IFN-γ production by allogeneic memory CD8⁺ T cells after coculture with IFN-γ–primed ECs transfected with control or p65 siRNA before addition of exogenous IL-1β or mock treatment. IFN-γ production was assessed by ELISA after 24 hours for coculture (72 hours after siRNA transfection). (**D**) Proliferation, activation, and granzyme B and perforin expression of CFSE-labeled CD8⁺ Tem cells after coculture with IFN-γ–primed ECs transfected with p65 or control siRNA and PRA or vehicle treatment for 6 hours. Flow cytometry analysis was performed on day 7. Data represent mean ± SEM. $^{**}P < 0.01$; $^{***}P < 0.001$; $^{****}P < 0.0001$; 1-way ANOVA and Tukey's multiple comparisons test. Representative of 3 to 4 independent experiments using 3 HUVEC donors.

MAC stabilization of endosomal NIK, activation of NLRP3 inflammasome, and IL-1β signaling drives translocation of nuclear IL-15/IL-15Rα complexes to the human EC cell surface. As noted in the Introduction, our prior work described a signaling pathway downstream of PRA binding to ECs that involved MAC formation and internalization, NIK stabilization on Rab5⁺MAC⁺ endosomes, endosomal NIK-mediated IL-1β synthesis and NLRP3 inflammasome assembly, IL-1β maturation and secretion, and IL-1 autocrine/paracrine activation of ECs. We next examined if this same pathway was responsible for PRA-induced IL-15/IL15Rα complex translocation from the nucleus to the cell surface. To identify which component(s) of the PRA sera induced nuclear translocation and IL-15/IL-15Rα surface expression, PRA sera was separated into IgG⁺ and IgG⁻ fractions. Neither the alloantibody-containing IgG⁺ fraction or complement-containing IgG⁻ fraction alone induced IL-15 and IL-15Rα surface expression on ECs (Figure 3A). IL-15 and IL-15Rα surface expression was reinduced when the IgG⁺ fraction was combined with complement-containing whole serum but not when combined with C9-deficient serum, indicating that alloantibody-mediated complement activation and MAC was necessary for the coordinate induction of surface IL-15/IL-15Rα complexes. To determine the extent to which MAC-mediated translocation of IL-15/IL-15Rα to the EC cell surface required IFN-γ priming, we deposited the same amount of MAC on the surfaces of unprimed and IFN-γ–primed ECs using an anti–human endoglin antibody that binds to an EC surface molecule not influenced by IFN-γ treatment, and assessed surface staining of IL-15 and IL-15Rα by flow cytometry (Figure 3B). We found that surface IL-15 and IL-15Rα expression were induced on ECs that had been IFN-γ pretreated and stimulated with MAC compared with control-treated ECs, separating the effects of the MAC-induced response from enhanced PRA binding. Rab5 GTPase activity is required to remodel endosomes in order to recruit and stabilize NIK protein. To determine if Rab5 GTPase activity is required for MAC induction of IL-15/IL-15Rα surface expression, ECs were stably transduced with a Rab5 dominant-negative (Rab5-DN) construct or Rab5 wild-type (Rab5-WT) construct. In ECs transduced with Rab5-WT construct, PRA treatment induced IL-15/IL-15Rα surface expression but not in ECs transduced with Rab5-DN, indicating that Rab5 activity was necessary (Figure 3C). Rab5 activity was not required for IFN-γ induction of IL-15 and IL-15Rα, as nuclear staining of both proteins was detected in vehicle-treated Rab5-WT and Rab5-DN ECs, indicating that Rab5 activity was involved only in the translocation process (Figure 3D). siRNA-mediated knockdown of NIK mRNA, which blocked stabilization of NIK and caspase-1 activation, also inhibited MAC-induced surface expression of IL-15 and IL-15R (Figure 3E and Supplemental Figure 3A). The induction of IL-15/IL-15Rα surface expression was abrogated with pharmacological inhibition of NLRP3 with MCC950, caspase-1 with Ac-YVAD-CMK or z-YVAD-FMK, and IL-1 binding to its receptor by blockade with IL-1 receptor antagonist (IL-Ra), indicating that NLRP3 inflammasome activation and IL-1 signaling are all also required for this process (Figure 3F). IL-1Ra also reduced the MAC-mediated induction of cell surface IL-15/IL-15Rα complexes as detected by PLA assay conducted between IL-15 and IL-15Rα on ECs (Figure 3G). Finally, MAC-induction of IL-15/IL-15Rα translocation was recapitulated by treating IFN-γ–primed ECs with IL-1β, which signals through canonical NF-κB signaling but not with treatment with LIGHT, a cytokine that activates noncanonical NF-κB by cytosolic NIK stabilization but does not activate an NLRP3 inflammasome or canonical NF-κB signaling (Figure 3H and Supplemental Figure 3B). Consistent with these findings, MAC-induced surface IL-15/IL-15Rα was significantly abrogated with inhibition of the EC response to IL-1β through blocking canonical NF-κB signaling by siRNA knockdown of p65 but not with inhibiting noncanonical NF-κB signaling with siRNA p100 (Figure 3I and Supplemental Figure 3C). Because TNF-α signaling through TNFR1 induces activation of the transcription factor NF-κB in human ECs (28), we examined the effects of TNF-α and found it also induced IL-15/IL-15Rα surface expression on IFN-γ–primed ECs (Supplemental Figure 4). These data collectively indicate that the MAC induction of nuclear translocation and IL-15/IL-15Rα induction on EC surfaces is mediated by the endosomal NIK, NLRP3 inflammasome, and IL-1β autocrine/paracrine signaling axis involving activation of the canonical NF-κB signaling.

Surface IL-15 on MAC-activated ECs is presented in trans and enhances allogeneic CD8⁺ Tem cell activation, proliferation, and differentiation. Having established that treatment of IFN-γ–primed human ECs can display IL-15/IL-15Rα complexes on their cell surface, we assessed if these complexes are functional by measuring the responses of allogeneic Tem cells. We previously reported that MAC/inflammasome/IL-1β signaling potentiated the ability of ECs to recruit and activate allogeneic CD4⁺ Tem cells. Here, IFN-γ–primed ECs were stimulated with PRA before coculture with either human allogeneic memory CD8⁺ or CD4⁺ Tem cells from the same PBMC donor, and responses were assessed after 7 days. As observed and reported before, PRA treatment significantly augmented allogeneic CD4⁺ Tem cell proliferation and activation that was inhibited with pretreatment of ECs with inhibitors of NLRP3, caspase-1 activity, and IL-1 receptor. We observed that anti–IL-15

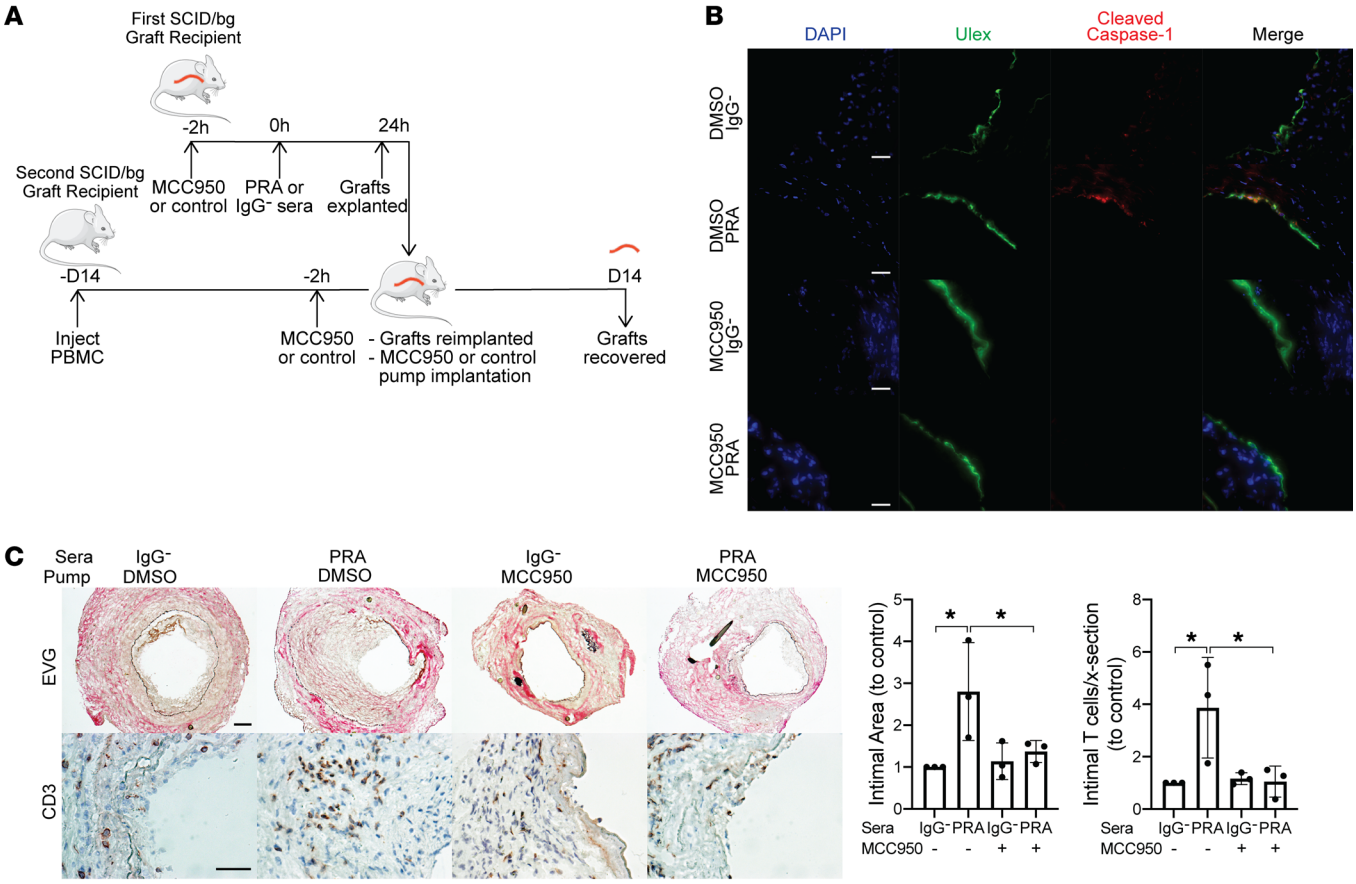

Figure 5. MCC950 blocks MAC-induced NLRP3 inflammasome activation by human ECs lining human artery xenografts and reduces the enhanced allogeneic memory T cell infiltration in vivo. (**A**) Human coronary artery grafts from a single donor were implanted into a set of 4 SCID/bg immunodeficient mice and quiesced for 7 days before pretreatment with NLRP3 inhibitor MCC950 or control DMSO in PBS before PRA or IgG⁻ sera treatment. After 24 hours, grafts were explanted and retransplanted into a second SCID/bg host with circulating allogeneic PBMCs. Osmotic pumps filled with MCC950 or DMSO in PBS were implanted subcutaneously in the second graft recipient at time of retransplantation. Grafts were recovered after 14 days. The experiment was repeated 3 times with different artery donors. (**B**) Human ECs lining arterial grafts were identified by Ulex staining and analyzed for cleaved caspase-1 staining by immunofluorescence. Scale bars: 50 μm. (**C**) Neointimal areas of grafts were assessed between treatment groups following EVG staining. Infiltrating intimal CD3⁺ T cells were identified and quantified following immunohistochemistry staining (n = 3). Scale bars: 50 μm. Data represent mean ± SEM. *P < 0.05, 1-way ANOVA and Tukey's multiple comparisons test. Results shown are representative of 3 artery grafts from 3 different artery donors.

blocking antibody had no effect on the CD4⁺ Tem cell response (Figure 4A). PRA treatment significantly enhanced allogeneic CD8⁺ memory T cell proliferation (as detected by CFSE dilution), activation (as measured by HLA-DR staining), and expression of effector molecules granzyme B and perforin (Figure 4B and Supplemental Figure 5). Inhibiting EC NLRP3 inflammasome assembly with MCC950, caspase-1 activation with z-YVAD-FMK, IL-1 receptor with IL-1Ra, or by preventing recognition of surface IL-15/IL-15Rα with anti–IL-15 blocking antibody, significantly reduced this augmentation of the CD8⁺ Tem cell proliferative response and effector molecule expression (Figure 4B). Neither CD8⁺ nor CD4⁺ Tem cells expressed surface IL-15 or IL-15Rα, indicating that the source of IL-15/IL-15Rα was from MAC-activated ECs (Supplemental Figure 6). To determine whether IL-1 signaling was acting on ECs or T cells, we performed siRNA knockdown of p65 in ECs to inhibit their responses to IL-1β, and added exogenous IL-1β to EC/CD8⁺ Tem cell cocultures. We observed that siRNA knockdown of p65 significantly attenuated the IFN-γ production by CD8⁺ Tem cells despite the availability of the added IL-1β to act on the T cells (Figure 4C). Knockdown of p65 in ECs also reduced the IL-1β–mediated augmentation of CD8⁺ Tem cell proliferation, activation, and differentiation (Figure 4D). Thus, the activation of the ECs largely mediated the effects of exogenous IL-1 on the allogeneic responses of CD8⁺ Tem cells, similar to what we had previously seen with CD4⁺ Tem cells. These results suggest that MAC/inflammasome/IL-1β pathway activates ECs to transpresent surface-bound IL-15 on IL-15Rα to allogeneic CD8⁺ Tem cells and enhanced CD8⁺ Tem cell activation, proliferation, and differentiation.

MCC950 blocks MAC-induced NLRP3 inflammasome activation and induction of IL-15/IL-15Rα transpresentation by human ECs lining human artery xenografts and reduces the enhanced allogeneic memory CD8⁺ T cell infiltration, proliferation, and differentiation in vivo. To determine if the effects on IL-15/IL-15Rα we have observed on cultured human ECs could be replicated in vivo, we used a human immune system mouse model. In this model, 4 approximately 1-mm diameter segments of epicardial human

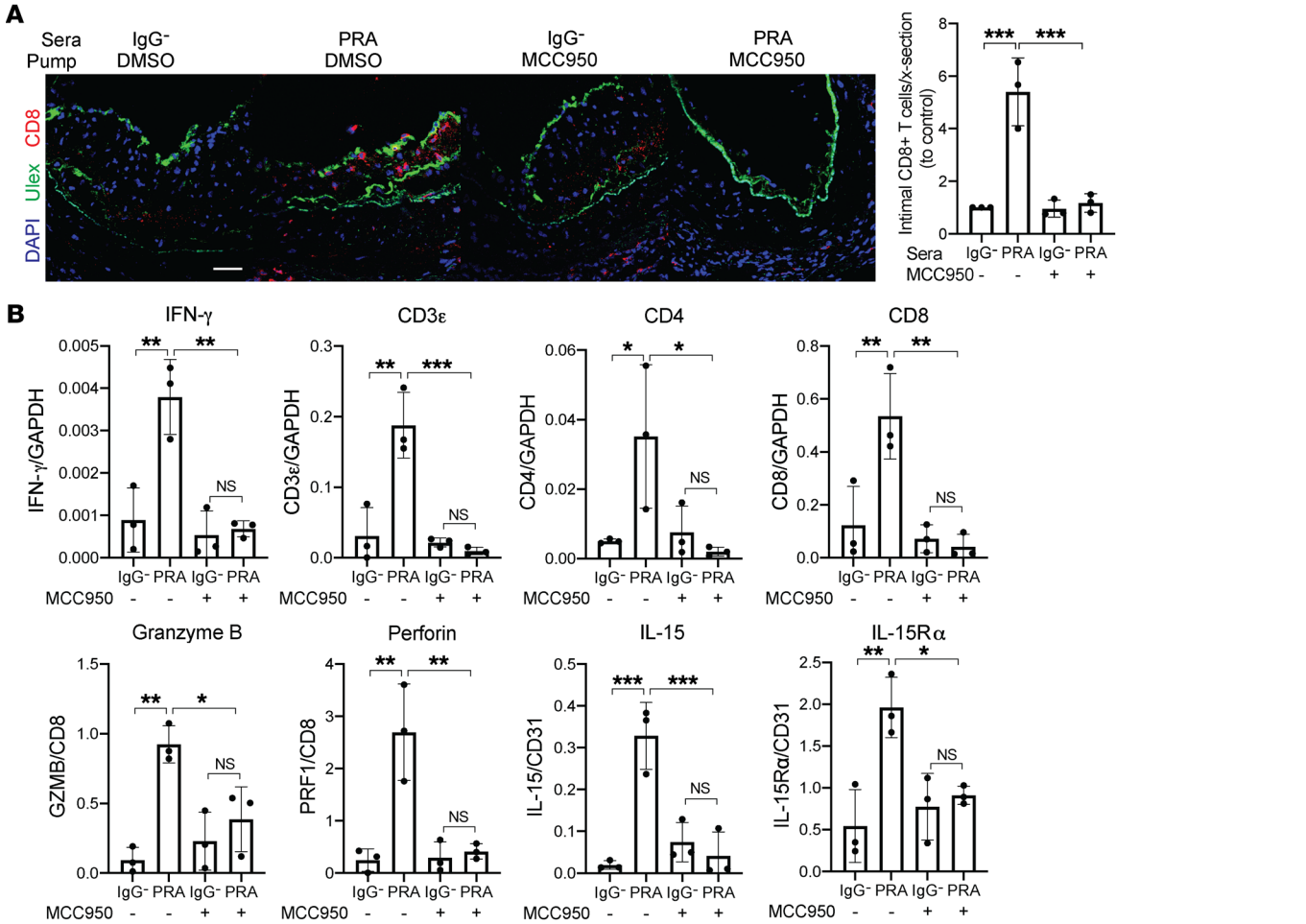

Figure 6. MCC950 blocks MAC-induced IL-15/IL-15Rα transpresentation by human ECs lining human artery xenografts and reduces the enhanced allogeneic memory CD8⁺ T cell infiltration, proliferation, and differentiation in vivo. (**A**) Artery grafts from Figure 6 were stained for Ulex to detect human endothelium and CD8. Infiltrating intimal CD8⁺ T cells were identified and quantified following immunofluorescence staining (n = 3). Scale bar: 50 μm. (**B**) qRT-PCR analysis of IL-15 and IL-15Rα (normalized to CD31); CD3ε, CD4, and CD8 (normalized to GAPDH); and granzyme B and perforin (normalized to CD8) in the grafts (n = 3). (**C**) Human ECs lining grafts were analyzed for IL-15 and IL-15Rα staining by immunofluorescence. Scale bar: 50 μm. Zoom shows higher magnification of the IL-15 and IL-15Rα staining of the human ECs lining the grafts, indicated by arrowheads, shown in the left panel. Scale bars: 10 μm. Note that IL-15 staining is increased in PRA-treated grafts, a change that is abrogated by MCC950, and that upon enlargement of the images, IL-15 staining is no longer confined to the nucleus of the ECs. Data represent mean ± SEM. *P < 0.05; **P < 0.01; ***P < 0.001; 1-way ANOVA and Tukey's multiple comparisons test. Results shown are representative of 3 artery grafts from 3 different artery donors.

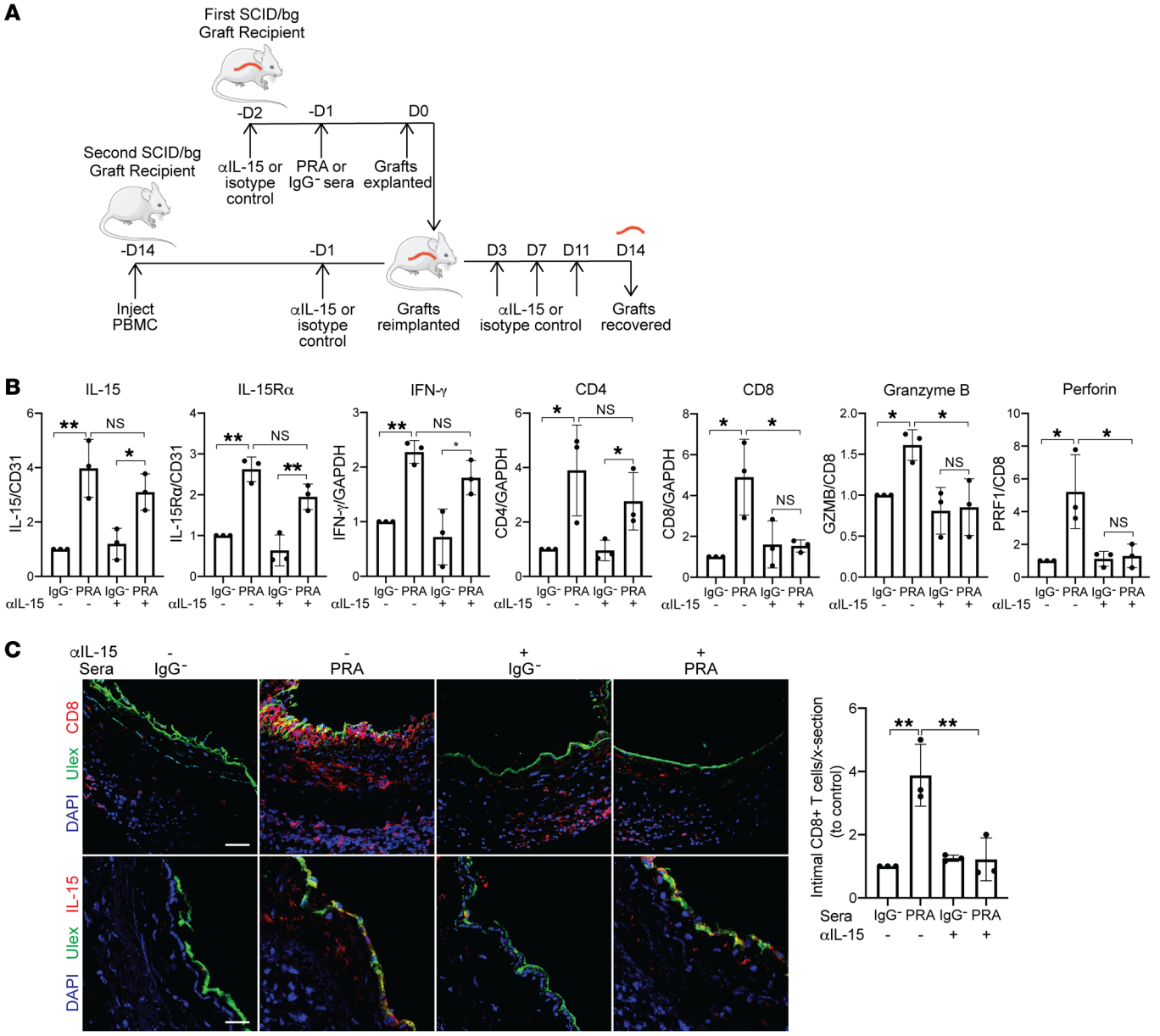

Figure 7. Anti–IL-15 blocking antibody reduces intimal CD8⁺ T cell infiltration and expression of effector molecules. (**A**) Human coronary artery grafts from the same donor were implanted into sets of 4 immunodeficient mice. Recipients were pretreated with anti–human IL-15 blocking antibody (αIL-15) or control isotype antibody before PRA or control sera treatment. Grafts were retransplanted into a second recipient with circulating allogeneic human PBMCs and similarly treated with anti–IL-15 blocking antibody or isotype control (n = 3). (**B**) qRT-PCR analysis of IL-15 and IL-15Rα (normalized to CD31); IFN-γ, CD4, CD8 (normalized to GAPDH); and granzyme B and perforin (normalized to CD8) in the grafts. Normalized expression is relative to isotype and IgG⁻ control group (n = 3). (**C**) Immunofluorescence detection of CD8 or IL-15 expression and human endothelium by Ulex in grafts. The intimal infiltrating CD8⁺ T cells were quantified. Scale bars: 50 μm. Data represent mean SEM. *P < 0.05; **P < 0.01; 1-way ANOVA and Tukey's multiple comparisons test. Results shown are representative of 3 artery grafts from 3 different artery donors.

coronary artery branches from a single donor, approximately 3–4 mm in length, are implanted, one segment per host, into sets of 4 C.B-17 SCID/bg immunodeficient mice as infrarenal aortic interposition grafts. The cells in these grafts remain of human origin, including a human EC lining of the lumen, and can be tested for responses to adoptively transferred elements of a human immune system. In a recently reported study, we allowed such grafts to quiesce for 7 days, at which time the graft recipient mice were pretreated with either NLRP3 inhibitor MCC950 or control DMSO in PBS, following which either PRA or control IgG⁻ sera injection (1 mouse per group of 4 for each combination) and grafts were harvested 24 hours later (12). We found that PRA induced both mouse complement deposition and inflammasome assembly in the EC lining, and that inflammasome assembly could be blocked by MCC950. In a further analysis of the same grafts, we failed to detect IL-15 and IL-15Rα or HLA-DR expression in the human EC lining, consistent with the absence of a human IFN-γ source in this experiment (Supplemental Figures 7 and 8).

Human ECs in situ express HLA-DR, consistent with basal stimulation by IFN-γ. Expression is lost by the ECs lining the arteries implanted into immunodeficient mouse hosts because mouse IFN-γ does not act on human cells (and vice versa) (29, 30). To test the effect of human IFN-γ on IL-15 and IL-15Rα expression in human ECs in vivo, we challenged implanted human artery segments that had been quiesced for 10 days by injecting the mice graft recipients with human IFN-γ or PBS control (Supplemental Figure 9A). The ECs lining freshly isolated human artery segments before graft transplantation not only express HLA-DR but also express IL-15 and IL-15Rα, consistent with basal IFN-γ priming of human ECs in situ (Supplemental Figure 9B). As detected by immunofluorescence staining of quiesced control artery segments, expression of all 3 proteins was lost within 10 days upon implantation into the mouse hosts (Supplemental Figure 9, B and C). Human IFN-γ treatment upregulated HLA-DR, IL-15, and IL-15Rα expression by human ECs lining the graft, as detected by immunofluorescence (Supplemental Figure 9, B and C). Analysis of the grafts by qRT-PCR also showed that human IFN-γ induced the expression of HLA-DR, IL-15, and IL-15Rα (Supplemental Figure 9D). Consistent with the in vitro data, these results indicate that human IFN-γ induces human ECs to upregulate IL-15 and IL-15Rα expression in vivo.

In a final series of experiments, we again used our transplant models to examine if the PRA effects on ECs that led to enhanced T cell responses observed in vitro also affected the allogeneic T cell response to ECs in vivo. We repeated the same initial treatments using the NLRP3 inhibitor MCC950 (Supplemental Figure 7) and then reimplanted the harvested grafts into a second set of 4 hosts that had been previously inoculated with human PBMCs allogeneic to the artery graft donor (Figure 5A). Simultaneously, an osmotic pump containing either MCC950 or control DMSO in PBS was implanted into each recipient subcutaneously depending on treatment group. Grafts were harvested after 14 days and analyzed. This experimental protocol avoided exposure of the adoptively transferred PBMCs to PRAs, and the groups receiving IgG-depleted sera allowed us to test the effect of MCC950 on an unmodified allogeneic T cell response to the grafts. As we described previously, the presence of human T cells in the circulation of the second set of hosts results in T cell infiltration of the graft vessel intima with expansion of the intimal area and concomitant luminal narrowing, providing a quantifiable model for human T cell–mediated graft rejection (11, 31). The experiment was repeated 3 times with different donors and the results were pooled for analysis. Cleaved caspase-1 staining, a marker of inflammasome assembly, was detected in human ECs lining the artery grafts exposed to PRA sera but not IgG^- control sera. MCC950 treatment inhibited PRA-induced EC NLRP3 inflammasome assembly (Figure 5B). Morphometric analyses revealed that intimal expansion and luminal narrowing were augmented in arteries exposed to PRA sera in the absence of MCC950 and enhanced intimal $CD3^+$ infiltrate (Figure 5C), consistent with prior findings. Analysis of the grafts by immunofluorescence showed that arteries exposed to PRA also had a more intense intimal $CD8^+$ T cell infiltration (Figure 6A), and qRT-PCR indicated an increase in IFN-γ, perforin, and granzyme B mRNA expression when normalized either to GAPDH, CD3ε, or CD8 mRNA (Figure 6B). Sustained release of MCC950 reversed the PRA-mediated augmentation, indicative of a role for inflammasome assembly. In the absence of PRA treatment, we detected low levels of IL-15 and IL-15Rα staining in the nuclei of human luminal ECs, consistent with the T cell–secreted IFN-γ (Figure 6C). The intensity of IL-15 and IL-15Rα staining and mRNA levels that are induced by PRA treatment is increased and correlated with the intensity of HLA-DR staining, consistent with the interpretation that a greater amount of IFN-γ is produced when T cells encounter MAC-activated allogeneic ECs (Figure 6, B and C, and Supplemental Figure 8). Although we are unable to unambiguously determine by confocal microscopy of harvested grafts if IL-15 or IL-15Rα have been translocated to the cell surface, PRA treatment induced extranuclear IL-15 and IL-15Rα staining and decreased nuclear staining in human graft ECs (Figure 6C). All of these changes induced by PRAs were dramatically reduced in animals receiving the NLRP3 inflammasome inhibitor. These observations support the interpretation that alloantibody and complement activation, via assembly of an NLRP3 inflammasome, function in vivo to enhance T cell recruitment and $CD8^+$ T cell maturation into CTLs, suggesting that transpresentation of IFN-γ–induced, IL-1–translocated IL-15/IL-15Rα complexes by human ECs contributes to these responses.

To establish that the inhibitory effects of MCC950-involved loss of IL-15 transpresentation, we next examined the effects of blocking recognition of EC-expressed PRA-activated IL-15/IL-15Rα on the allogeneic T cell response in vivo. Artery graft recipient mice were pretreated with either anti–IL-15 blocking antibody or isotype control antibody before either PRA or control IgG^- sera injection (1 mouse per group of 4 for each combination). Grafts were retransplanted 24 hours later into recipients with adoptively transferred human allogeneic PBMCs and continued to be treated with either anti–IL-15 blocking antibody or isotype control (Figure 7A). As observed previously, PRA treatment in anti–IL-15 or isotype control antibody groups induced higher IL-15 and IL-15Rα staining colocalizing with human EC lining and mRNA levels, consistent with the greater amounts of T cell–secreted IFN-γ in the graft (Figure 7, B and C). However, anti–IL-15 blocking antibody reduced the augmented number of intimal infiltrating $CD8^+$ T cells and $CD8^+$, granzyme B, and perforin mRNA levels, but not $CD4^+$, consistent with in vitro results (Figure 7, B and C). These results collectively indicate that blocking the recognition of IL-15 complexes on PRA-activated ECs lining human artery xenografts inhibited IL-15 transpresentation by ECs to $CD8^+$ T cells and diminished $CD8^+$ proliferation and differentiation.

Discussion

Vascular endothelium plays a major immunologic role in tissue homeostasis. Allograft ECs are a principal source of nonself MHC class I and class II molecules and are therefore a primary target of both recipient humoral and cellular alloimmune responses. Acute rejection is largely mediated by host effector memory $CD8^+$ T cells that directly recognize nonself class I MHC molecules complexed to many different peptides expressed by the graft ECs. Graft ECs recruit and activate alloreactive $CD8^+$ Tem cells and induce $CD8^+$ Tem cell transendothelial migration and maturation into effector CTLs within the allograft. $CD4^+$ Tem cells help promote CTL dif-

ferentiation and survival by releasing IL-2 and other mediators (5). The development of preformed complement-fixing donor-specific antibodies (i.e., PRA), most often complement-fixing and directed toward nonself MHC alleles, is a risk factor for and precipitates acute rejection. Our findings here are part of our ongoing efforts to study how alloantibody and complement-mediated intracellular signaling enhances EC immunogenicity and the ability of ECs to recruit and activate Tem cells, linking alloantibody to T cell–mediated acute and chronic rejection.

Using in vitro and in vivo models of human ECs and allogeneic T cell responses, we elucidate how MAC signaling induces IFN-γ–primed ECs to traffic their nonsecreted nuclear IL-15/IL-15Rα protein complex stores to the cell surface for transpresentation to $CD8^+$ Tem cells, potentiating CTL development. Key new findings of this study are that internalized MAC stabilization of endosomal NIK, activation of the NLRP3 inflammasome, secretion of IL-1β, and autocrine/paracrine activation of canonical NF-κB pathway stimulate nuclear translocation of IL-15/IL-15Rα complexes for display and transpresentation on the EC cell surface. While IFN-γ induces expression of unoccupied IL-15Rα on the cell surface, IFN-γ primes ECs for coordinate surface expression of IL-15/IL-15Rα by upregulating IL-15 and IL-15Rα protein expression in the nucleus, where IL-15 is associated with IL-15Rα. Upon MAC signaling in IFN-γ–primed ECs, EC-derived IL-15 bound to IL-15Rα translocates from the nucleus to the cell surface where it can be presented in *trans* to alloimmune $CD8^+$ Tem cells, promoting activation and proliferation, and IFN-γ, granzyme B, and perforin effector molecule expression, characteristic of CTL development. Consistent with in vitro results, we showed that human ECs lining quiesced artery grafts implanted in immunodeficient mice in the absence of a source of human IFN-γ lose HLA-DR, IL-15, and IL-15Rα expression compared with pretransplant graft segments. The expression of these molecules are reinduced upon human IFN-γ treatment. Using an in vivo model of human T cell responses to allogeneic vascular cells, we demonstrate that IL-15 and IL-15Rα expression were induced in the presence of greater T cell–derived human IFN-γ production. Alloantibody and complement treatment of human ECs lining an artery xenograft led to increased IL-15/IL-15Rα expression on human ECs and potentiated T cell–mediated graft injury with enhanced CTL development of infiltrating intimal $CD8^+$ Tem cells. Blockade of NLRP3 inflammasome assembly and IL-15/IL-15Rα induction on ECs with MCC950 appeared to protect the allograft arteries and the EC-reactive $CD8^+$ Tem cell expansion and effector differentiation. Furthermore, inhibiting EC-derived IL-15 transpresentation by blocking the recognition of IL-15/IL-15Rα on PRA-treated MAC-activated graft ECs with an anti–IL-15 blocking antibody abrogated the augmented allogeneic $CD8^+$ intimal infiltration and CTL development.

IL-15 is known to be critical in supporting proliferation and activity of $CD8^+$ memory T cells. While IL-15 transcript has been observed to be more widely and abundantly produced in various tissues and cell types, IL-15 protein is produced at very low levels by a limited number of cells during periods of immune response and inflammation (22). This discordance between transcript and protein expression is suggestive of tight intracellular regulation and trafficking of IL-15 in response to inflammatory activators. Very little IL-15 is secreted. Instead, IL-15 is presented as a complex with IL-15Rα expressed on the surface of one cell in *trans* $CD8^+$ T cells or NK cells expressing IL-2Rβ/γ_c. IL-15 signaling and production have been largely studied in activated macrophages, monoctyes, and DCs, in which others have reported that transcriptional regulation of IL-15 depends on NF-κB, interferon regulatory factor 1 (IRF-1), and IRF-3 binding to the 5′ regulatory region of IL-15 (32). Our findings additionally suggest a possible intracrine role for nonsecreted IL-15 in ECs, in which transcript and nuclear IL-15 and IL-15Rα protein expression is induced by IFN-γ. The association of nuclear IL-15 with nuclear IL-15Rα in complex detected by PLA is unexpected and we believe it is novel. IFN-γ upregulation of unoccupied IL-15Rα on EC surfaces is consistent with previous reports that IFN-γ treatment enhances the ability of human ECs to bind and elaborate added exogenous IL-15, implicating that ECs have the ability to capture IL-15 from solution (26). However, we demonstrate that IFN-γ–primed ECs can be induced by MAC signaling and IL-1β through activation of canonical NF-κB signaling to traffic its nuclear IL-15/IL-15Rα protein complex stores for coordinate cell surface expression. The MAC/NLRP3 inflammasome/IL-1β signaling axis triggers nuclear translocation and display of EC-derived IL-15/IL-15Rα on the cell surface, available for transpresentation. This process is dependent on activation of the canonical NF-κB pathway, as IL-1β or TNF-α treatment of IFN-γ ECs could stimulate IL-15/IL-15Rα translocation but not LIGHT, a cytokine activator of noncanonical NF-κB signaling. It seems likely that translocation of IL-15/IL-15Rα complexes from nucleus to cell surface depends upon synthesis of a new protein that is induced in response to canonical NF-κB–mediated transcription, but the identity of this protein (or proteins) is currently unknown and a subject for further investigation. In experiments by Dubois et al. where soluble IL-15 was added to cultures of activated monocytes expressing IL-15Rα to allow IL-15/IL-15Rα transpresentation, endosomal recycling of IL-15/IL-15Rα from the cell surface allowed for plasma membrane-bound IL-15 to persist even after the withdrawal of IL-15 from the medium or a short stripping treatment of surface IL-15 (18). The possibility of recycling of either IL-15 or IL-15Rα from the cell surface and the mechanism in human ECs after nuclear translocation and induction of cell surface IL-15/IL-15Rα are also subjects for future investigation.

A recent report has shown that in a mouse tumor model, IL-1β can enhance the response of adoptively transferred CTL-mediated killing in a manner dependent upon IL-2 and IL-15 (27). Conditional deletion of IL-1R1 from ECs using a cadherin 5-*Cre* transgene abrogated the effect, consistent with the data reported here using human cells. While the authors of this study correlated the IL-1 effect with an increase in IL-15Rα splenic neutrophils, a simpler explanation may be transpresentation of IL-15 by mouse ECs. However, there may well be species differences and the use of human materials in our work and models allows us to gain relevant insights into mechanisms of transplant rejection that are not well reproduced in mice. More specifically, human ECs are effective at alloantigen presentation to both $CD4^+$ and $CD8^+$ Tem cells, populations lacking in commonly used mouse graft recipients, but are unable to activate naive T cells. Mouse ECs do not activate $CD4^+$ effector T cell responses but do express CD86 and

can present alloantigen to naive CD8+ T cells. Antigen-presenting functions are important to understand IL-15 actions because IL-15 delivers signaling to target cells in the context of cell-to-cell contact together with costimulatory molecules at the immunological synapse to modify the response of the cell (15, 23). In human transplantation, CD8+ Tem cells can home directly into allografts and mature into CTL within the grafts, bypassing secondary lymphoid organs. The roles of CD8+ Tem cells and graft ECs can be successfully modeled in vivo using humanized mice. Our findings that inhibiting complement-mediated NLRP3 inflammasome activation and induction of IL-15 transpresentation on ECs with MCC950 blocks the potentiated CD8+ Tem cell response and CTL development points to potentially druggable molecular targets. Targeting vascular EC MAC signaling by blocking NLRP3 inflammasome, IL-1β or IL-15 signaling may be beneficial for sensitized transplant patients with complement-fixing antibodies.

Antibody binding and complement activation leading to EC injury and activation occur in many other clinical settings. For instance, the majority of patients with allograft vasculopathy (AV), a major cause of late graft failure, have formed donor-specific antibodies, most often complement-fixing and directed against nonself class II MHC, that lead complement activation and signaling by graft ECs. Although the role of CD8+ Tem cells in AV pathogenesis is unclear, NK cells have been implicated as mediators of graft damage in allograft vasculopathy by engaging donor-specific antibodies bound to graft ECs. NK cells are effectors of antibody-dependent cytotoxicity (ADCC), which can be enhanced by IL-15 (33, 34). IL-15 transpresentation by ECs to NK cells may promote allograft vasculopathy pathogenesis by enhancing NK cell activation and cytolytic activity. Activation of complement and EC activation has long been recognized in atherosclerosis, Alzheimer's, and immune complex-mediated diseases, including small vessel vasculitis (35–37). Antibody and complement may also be important for tumor immunity or for cytolytic forms of autoimmunity, such as type I diabetes. In these settings, complement-mediated EC activation and IL-15 transpresentation may augment CD8+ T cell recruitment, activation, and cytotoxicity. While the therapeutic benefit of complement inhibitors is being actively studied in these settings, targeting more specific mediators of inflammatory damage such as the inflammasome, IL-1β, or IL-15 signaling may be more effective in controlling the disease pathology.

Methods

Cell isolation and culture. All protocols involving collection of and experimentation with human cells and tissues were approved by the Yale University Institutional Review Board. Human umbilical vein ECs (HUVECs) were isolated from deidentified umbilical cords following enzymatic digestion by collagenase. Cells used in all experiments were serially cultured at 37°C on 0.1% gelatin-coated (MilliporeSigma) tissue culture plates in endothelial cell growth medium (EGM2, Lonza) and used for experiments between passage levels 1 to 6. Leukapheresis products were collected from healthy adult volunteers in the Yale blood bank and then deidentified before transfer to the laboratory. Mononuclear cells were enriched by density gradient centrifugations using lymphocyte separation medium (MP Biomedical, 50494X) per the manufacturer's instructions and cryopreserved in 10% DMSO/90% FBS in liquid nitrogen. Thawed cells were washed in RPMI (Gibco) supplemented with 5% FBS, 1.5% L-glutamine, and 1% penicillin/streptomycin. Human CD8+ and CD4+ T cells were isolated from total PBMCs by positive selection with magnetic Dynabeads CD8 (Invitrogen, 11333D) and Dynabeads CD4 (Invitrogen, 11331D), respectively, per the manufacturer's protocol and released with Detachabeads in the Dynabeads Positive Isolation kit (Invitrogen, 11333D and 11331D). Resting effector memory (CCR7-HLA-DR-) T cells were purified from total CD8+ and CD4+ T cells by negative selection using anti–human CCR7 antibody (BioLegend, 353222) and HLA-DR antibody (BioLegend, 307602) by magnetic separation with Dynabeads Pan Mouse IgG (Invitrogen, 11041) to remove antibody-bound cells. The final population was identified as 90% to 98% resting CD8+ and CD4+ effector memory T cells by flow cytometry analysis.

Viral transduction of ECs. Retroviral vector encoding mCherry-Rab5WT was generated, as described previously, by cutting mCherry-Rab5WT vector (Gia Voeltz, University of Colorado at Boulder, Boulder, Colorado, USA; Addgene plasmid 49201) at the BamH1 and Not1 sites and ligated into the retroviral expression vector pLZRSpBMN-Z (gift from Garry Nolan, Stanford University, Stanford, California, USA) (12). Retroviral vector encoding mCherry-Rab5DN was generated by using PCR and primer sequence GCGGCCGCTCAGTTACTACAACACTGATT to introduce a 3′ Not1 restriction site using the mCherry-Rab5DN (S34N) vector (Sergio Grinstein, University of Toronto, Toronto, Ontario, Canada; Addgene plasmid 35139) as template and the insert was cut with BamH1 and Not1 and then ligated into pLZRSpBMN-Z. Constructs were confirmed by sequencing (Yale Keck Sequencing Facility). To generate retrovirus encoding Rab5WT or Rab5DN, Phoenix cells (gift from Garry Nolan, Stanford University, Stanford, California, USA) were transfected using Lipofectamine 2000 with the retroviral plasmids encoding Rab5-WT and Rab5-DN. Viral supernatants were collected and used to transduce HUVECs as described above.

Antibody and complement treatment of ECs. Discarded, deidentified, and pooled preparations of high-titer PRA sera from transplant candidates that showed more than 80% reactivity to class I and II MHC antigens were collected from the Yale New Haven Hospitals' tissue typing laboratory. In vitro studies of EC response to complement were elicited using high titer PRA in gelatin veronal buffer (GVB, MilliporeSigma, G6514) to treat serially passaged HUVEC cultures. Where indicated, PRA sera was separated into IgG+ and IgG– fractions as described previously using the MAbTrap kit (GE Healthcare, 17-1128-01) according to the manufacturer's instructions (11, 12). IgG+ and IgG– fractions were serially concentrated using 3 kDa Amicon-Ultra-4 Centrifugal Filter Units (MilliporeSigma) and brought to a final volume equal to the total PRA volume before sera fractionation (11). Normal human sera and C9-deficient sera were purchased from Quidel Corporation (A505) and MilliporeSigma (S1764). Unless otherwise indicated, HUVECs were treated with IFN-γ (50 ng/mL, Gibco, PHC4033) for 48 hours in EGM2 media before treatment with PRA to reinduce class I and class II MHC expression. Where indicated, HUVECs were treated with 1 μM MCC950 (Cayman Chemical), 20 μM Ac-YVAD-CMK (Cayman Chemical, 178603-78-6), 20 μM z-YVAD-FMK (Biovision, 1141-5), 10 μg/mL IL-1 receptor antagonist (PeproTech, 200-01RA), 20 μg/mL anti–IL-15 blocking antibody (R&D Systems, MAB247), or DMSO in GVB for 30 minutes, at the indicated concentrations, before PRA treatment. PRA was subsequently added to ECs in GVB at a 1:3 ratio for 30 minutes or 4 hours. To separate the effects of MAC and

IFN-γ priming, ECs were treated with 50 ng/mL IFN-γ or mock treated for 48 hours before incubation with either 20 μg/mL of anti-human endoglin IgG_{2A} antibody (Santa Cruz Biotechnology, P3D1) or isotype control with human complement (MilliporeSigma, S1764) for 4 hours. HUVECs were treated with 100 ng/mL LIGHT (R&D Systems, 664-LI-025) for 18 hours, 100 pg/mL recombinant IL-1β (Thermo Fisher Scientific, 10139HNAE5) for 6 hours, and 10 ng/mL TNF-α (R&D Systems, 210-TA) for 6 hours. After treatment, ECs were washed with PBS and analyzed as indicated in figures and described below. Supernatants were collected for ELISA analysis.

Small interfering RNA (siRNA) knockdown of EC proteins. HUVECs were transfected with 20 nM (Dharmacon, LQ-003580-00-0002), NFKB2 (Dharmacon, L-003918-00-0005), RELA (Dharmacon, L-003533-00-0005), or control nontargeting 1 (Dharmacon, D-001810-01-05) with RNAiMax (Invitrogen), according to the manufacturers' instructions for 18 hours. IFN-γ (50 ng/mL) was added to transfected cultures the following day for 48 hours unless otherwise indicated before treatment with PRA sera or GVB. Successful knockdown was confirmed by immunoblotting.

Subcellular fractionation and immunoblot analysis. To extract and prepare cytoplasmic, membrane, nuclear soluble, and chromatin-bound proteins for immunoblot analysis, EC lysates were harvested by a stepwise lysis using the Subcellular Protein Fractionation Kit for Cultured Cells (Thermo Fisher Scientific, 78840) according to the manufacturer's instructions. For whole-cell lysate analysis, ECs were washed with ice-cold PBS twice after treatment and were lysed in RIPA buffer (Cell Signaling Technology, 9806). Laemmli buffer (Bio-Rad) and 0.1 M dithiothreitol (MilliporeSigma) were added to protein lysates, heated at 95°C for 10 minutes, run on precast protein gels (Bio-Rad), and transferred to PVDF membrane (Bio-Rad). Membranes were blocked in 5% BSA in TBS-T for 1 hour at room temperature. Primary antibodies were used in 1:1000 dilution with incubation overnight at 4°C. Antibodies included: IL-15 (Santa Cruz Biotechnology, sc-8437), IL-15Rα (R&D Systems, AF247), Hsp90α/β (Santa Cruz Technology, sc-13119), calnexin (Cell Signaling Technology, 2679), lamin A/C (Santa Cruz Technology, sc-6215), histone H3 (Cell Signaling Technology, 4499), p100/52 (Cell Signaling Technology, 37359S), caspase-1 (Santa Cruz Biotechnology, sc-622), p65 (Santa Cruz Biotechnology, sc-8008), phospho-p65 (Cell Signaling Technology, 3033S), NIK (Cell Signaling Technology, 4994S), beta-actin (Cell Signaling Technology, 4970S). Membranes were washed and incubated with the appropriate secondary antibody in a 1:10,000 dilution for 1 hour at room temperature. Secondary antibodies used were peroxidase–AffiniPure Goat Anti-Rabbit IgG (H+L) (Jackson ImmunoResearch, 111-035-144) and Peroxidase–AffiniPure Goat Anti-Mouse IgG (H+L) (Jackson ImmunoResearch, 115-035-062). Bound HRP was visualized using Super-Signal Femto or Pico West (Pierce) and chemiluminescent x-ray films (Denville Scientific) were developed using a Konica Minolta SRX-101A film processor. Densitometry was performed and analyzed using National Institutes of Health ImageJ software.

Proximity ligation assay. ECs were cultured on 0.1% gelatin-coated coverslips in 24-well tissue culture plates. After indicated treatments, ECs were washed with Hanks Balanced Salt Solution (HBSS, Gibco) twice. For conducting PLA between cell surface proteins, primary antibodies were added at 5 μg/mL in EGM2 media at 37°C for 20 minutes. ECs were washed with PBS and fixed with 2% paraformaldehyde in PBS for 20 minutes at room temperature. After washing with PBS 3 times, samples were blocked with Duolink Blocking Solution (MilliporeSigma, DUO82007) for 60 minutes at 37°C. For conducting PLA between intracellular proteins, ECs were fixed and permeabilized with ice-cold methanol for 15 minutes before blocking and primary antibody incubation for 1 hour. Primary antibodies included IL-15 (Santa Cruz Biotechnology, sc-8437), IL-15Rα (R&D Systems, AF247), and Histone H1 (Santa Cruz Biotechnology, sc-8030). PLA assay was performed using Duolink flowPLA Detection Kit, Far Red (MilliporeSigma, DUO94004). After washing with PBS twice for 5 minutes at room temperature, samples were incubated with PLA probes in PLA antibody diluent (MilliporeSigma, DUO82008) for 60 minutes at 37°C. Probes used were the Duolink In Situ PLA Probe Anti-Mouse MINUS (MilliporeSigma, DUO924004) and Duolink In Situ PLA Probe Anti-Goat PLUS (Sigma-Aldrich, DUO92003). Samples were washed with PBS twice for 5 minutes at room temperature and ligase (MilliporeSigma, DUO82027) in ligation buffer (MilliporeSigma, DUO82009) was added to samples for 30 minutes at 37°C. After washing twice with PBS, samples were incubated with polymerase (MilliporeSigma, DUO82028) in amplification buffer (MilliporeSigma, DUO82050) for 100 minutes at 37°C. Samples were washed with PBS twice and detection solution (MilliporeSigma, DUO84004) was added for 30 minutes protected from light at 37°C. Samples were washed twice with Wash Buffer B (1×, MilliporeSigma, DUO82048) at room temperature for 10 minutes, Wash Buffer B (0.01×, MilliporeSigma, DUO82048) at room temperature for 1 minute and mounted using ProLong Gold Mounting Reagent with DAPI (Life Technologies). Confocal images were acquired on the Leica TCS SP5 using LAS AF software and ×63 oil objective.

Immunofluorescence staining of cultured ECs. ECs were cultured on 0.1% gelatin-coated coverslips in 24-well tissue-culture plates. For staining of cell-surface proteins, ECs were washed twice with HBSS (Gibco) after indicated treatments, and primary antibody was added at 5 g/mL in EGM2 for 20 minutes at 37°C. After washing off excess antibody with PBS, ECs were fixed with fresh 2% paraformaldehyde in PBS for 20 minutes, and blocked with 5% donkey serum in PBS for 1 hour at room temperature. For staining of intracellular proteins, ECs were fixed and permeabilized with ice-cold methanol, blocked with 5% donkey serum in PBS/0.01% Tween for 1 hour at room temperature, and incubated with primary antibodies overnight at 4°C. Primary antibodies include IL-15 (Santa Cruz Biotechnology, sc-8437) and IL-15Rα (R&D Systems, AF247). All samples were incubated for 1 hour at room temperature with the appropriate Alexa Fluor–conjugated and high-cross–absorbed secondary antibodies in 5% donkey serum/0.01% Tween/PBS blocking solution (1:500 dilution).

T cell activation assays. ECs were cultured on 96-well round bottom plates and pretreated with IFN-γ for 48 hours. Where indicated, HUVECs were treated with 1 μM MCC950 (Cayman Chemical), 20 μM Ac-YVAD-CMK (Cayman Chemical, 178603-78-6), 20 μM z-YVAD-FMK (Biovision, 1141-5), 10 μg/mL IL-1 Receptor Antagonist (PeproTech, 200-01RA), 20 μg/mL anti–IL-15 blocking antibody (R&D Systems, MAB247), or DMSO in GVB for 30 minutes, before treatment with PRA sera or GVB control for 6 hours. Freshly isolated human $CD8^+CCR7^-$HLA-DR^- and $CD4^+CCR7^-$HLA-DR^- T cells were cocultured with the allogeneic HUVECs at a EC/CD8 and EC/CD4 T cell ratio of 1:30 and 1:20, respectively, in RPMI 1640 media supplemented with 10% FBS, 2% L-glutamine, 1% penicillin. T cell proliferation was assayed by labeling T cells using the Cell Trace CFSE

Proliferation Kit (Invitrogen, C34554) and assessed by flow cytometry after 7 days. On day 1 of coculture, 100 pg/mL recombinant human IL-1β (Thermo Fisher Scientific, 10139HNAE5) or vehicle control was added where indicated. Supernatants were collected after 24 hours of coculture (72 hours after siRNA transfection) for cytokine secretion that was assayed by ELISA.

Flow cytometry analysis. To assess cell-surface expression and complement binding, treated ECs were suspended with trypsin versene, washed and incubated with a Fixable Viability Dye (eBioscience, 65-0865-14), anti–human IL-15 (R&D Systems, IC2471A), anti–human IL-15Rα (R&D Systems, AF247), anti–human C5b-9 (Dako, M077701-5), and anti–human HLA-DR (BioLegend, 307622), at 1:50 dilution in 1% BSA/PBS, and analyzed. After 7 days of EC/T cell coculture, T cell proliferation, activation, and cytokine production were assessed by flow cytometry. T cells were harvested and stained with Fixable Viability Dye (eBioscience, 65-0865-14), anti–human CD4 (BioLegend, 317424), anti–human CD8 (eBioscience, 48-0086-42), and anti–human HLA-DR (BioLegend, 307676). For intracellular cytokine staining, samples were fixed and permeabilized using Intracellular Fixation and Permeabilization Buffers (eBioscience, 88-8824-00) according to the manufacturer's instructions, and staining was performed using anti–human perforin (BioLegend, 308110) and anti–human granzyme B (BD Pharmingen, 561142). CFSE dilution was assessed as an indicator of proliferation. All samples were acquired using the BD LSRII Flow Cytometer and BD FACSDiva Software and analyzed with FlowJo software.

Measurement of cytokine production. Supernatants collected from complement-treated ECs were analyzed for IL-15 using human IL-15 DuoSet ELISA (R&D Systems, DY247). Freshly isolated human $CD8^+CCR7^-HLA\text{-}DR^-$ T cells were cocultured with HUVECs that had been transfected with siRNA as indicated and treated with IFN-γ for 48 hours. After 24 hours of coculture (or equivalently 72 hours after siRNA knockdown), supernatants were collected and assayed by ELISA using human IFN-γ ELISA Ready-SET-Go! (eBioscience, 88-7316-88).

Human artery graft transplantation and recipient treatment. All protocols involving animals were approved by the Yale Institutional Animal Care and Use Committee. Human coronary arteries of approximately 0.8 mm in diameter, from the native hearts of deidentified transplant recipients or from organ donors whose hearts were not used for transplantation, were interposed into the descending infrarenal aorta of female C.B-17 SCID/beige mice (Taconic Biosciences). The transplanted arteries were quiesced for 7 to 10 days.

Where indicated, mice were injected i.p. with vehicle (DMSO) or 5 mg/kg MCC950 (Cayman Chemical, 17510). After 2 hours, mice were injected i.v. with 200 μL neat PRA sera or IgG^- sera. Artery grafts were retransplanted after 24 hours into a second SCID/beige host that had received 2×10^8 human allogeneic PBMCs i.p. 2 weeks before retransplantation (31). At the time of retransplantation, an osmotic pump (Alzet 2002, 0000296) filled and primed according to the manufacturer's instructions to deliver 5 mg/kg/day of MCC950 or DMSO/PBS was implanted subcutaneously at a midscapular position. Alternatively, where indicated, mice were injected i.p. with anti–IL-15 blocking antibody (R&D Systems, MAB 247) or irrelevant IgG_1 antibody (MOPC 21, MP Biomedicals, 50327) starting with a 200 μg loading dose 24 hours before PRA sera or IgG^- sera injection and retransplantation. Retransplanted graft recipients were subsequently treated with a 100 μg dose every 4 days. Successful engraftment of human $CD3^+$ T cells, achieved in all mice in this study, was defined as 1% to 10% human $CD3^+$ T cells engraftment relative to total murine $CD45^+$ leukocytes before artery graft retransplantation as assessed by flow cytometry analysis of peripheral blood sampled. Retransplanted artery grafts were explanted with cuffs of mouse aorta on both ends and then interposed into the infrarenal aortae of a second recipient (31). After 14 days, retransplanted artery grafts were recovered, embedded, and snap-frozen in OCT and sectioned at 5-μm thickness.

Where indicated, after transplanted grafts were quiesced for 10 days, graft recipients were injected with human recombinant IFN-γ (Gibco, PHC4031) or sterile PBS (Gibco, 14190-144) at 600 ng s.c. twice every 24 hours before harvesting at 72 hours and embedding grafts in OCT.

Microscopic analysis of artery grafts. Cross-sections of 5-μm thick artery grafts were fixed in ice-cold acetone for 15 minutes, washed with PBS, blocked in 5% donkey serum in PBS-T, and incubated with Ulex Europaeus Agglutinin I-Fluorescein labeled (1:200, Vector, RL-1061), poly-C9 (1:100, Dako M077701-5), cleaved caspase-1 (1:100, Cell-Signaling Technology, D57A2), CD8 (1:100, BioLegend, 344702), IL-15 (1:100, Santa Cruz Biotechnology, sc-8437), IL-15Rα (1:100, R&D Systems, AF247), or HLA-DR (1:100, BioLegend, 307602) overnight at 4°C. Samples were washed with PBS and incubated with the appropriate Alexa Fluor secondary antibody (1:500) for 1 hour at room temperature before being coverslipped and mounted. Fluorescence images were acquired using Volocity software and the ×20 objective filter on the Axiovert 200M microscopy system (Carl Zeiss MicroImaging) epifluorescence microscope. Confocal images were acquired on the Leica TCS SP5 using LAS AF software and ×63 oil objective. Microscopic morphometric evaluation was performed on Elastica-van Gieson–stained (EVG-stained) 5-μm artery graft sections using ImageJ software. Graft-infiltrating human lymphocytes were quantified by staining for human CD3 (BioLegend, 344802) using the avidin-biotin-peroxidase staining method (Vector Laboratories). Histology images were acquired on EVOS FL Auto2.

Real-time quantitative reverse transcription–polymerase chain reaction (qRT- PCR). Total RNA was isolated from artery grafts by resuspending serial sections of artery grafts in RLT lysis buffer (Qiagen). RNA was isolated from ECs or grafts using the RNeasy kit (Qiagen) according to the manufacturer's protocol. RNA was reverse transcribed to cDNA using the high-capacity cDNA Reverse Transcription kit (Applied Biosystems, 4368814). cDNA was amplified using the TaqMan gene expression Master Mix (Applied Biosystems, 4369016), and TaqMan gene expression probes (Applied Biosystems), including IL15 (Hs01003716_m1), IL15RA (Hs00542602_g1), CD8A (Hs00233520_m1), CD4 (Hs01058407_m1), CD3E (Hs01062241_m1), PECAM1 (Hs01065279_m1), GZMB (Hs00188051_m1), PRF1 (Hs00169473_m1), HLA-DR (Hs00219575_m1), CASP1 (Hs00354836_m1), and GAPDH (Hs02786624_g1). Reactions were run on a CFX96 real-time system using CFX Manager Software (Bio-Rad). Gene expressions were normalized to GAPDH unless otherwise indicated.

Statistics. Data are expressed as mean ± SEM. Statistical analyses were performed using GraphPad Prism software. As indicated in the figure legends, unpaired 2-tailed Student's *t* tests were used to make statistical comparisons between 2 groups. Comparisons between

multiple groups were performed by 1-way ANOVA with Tukey's test for post hoc analysis. A *P* value of less than 0.05 was considered statistically significant.

Study approval. All protocols involving collection of and experimentation with human cells and tissues were approved by the Yale University Institutional Review Board (New Haven, Connecticut, USA). All experiments involving animals were conducted according to protocols approved by the Yale University Institutional Animal Care and Use Committee (New Haven, Connecticut, USA).

Author contributions

CBX and JSP conceived the research studies and analyzed data. CBX, BJ, LQ, NCKS, GT, and DJW conducted experiments, acquired data, and/or contributed new reagents. CBX and JSP wrote the manuscript.

Acknowledgments

We thank Gwendolyn Davis-Arrington for HUVEC isolation. This work was supported by NIH R01-HL051014 and U01-AI132895 (to JSP), NIH R01-HL141137 (to DJ), and NIH F30-AI138473 and NIH MSTP T32-GM007205 (to CBX).

Address correspondence to: Jordan S. Pober, 10 Amistad Street, New Haven, Connecticut 06509, USA. PO Box 208089, New Haven, CT 06520-8089, USA. Phone: 203.737.2292; Email: jordan.pober@yale.edu.

1. Abrahimi P, Liu R, Pober JS. Blood vessels in allotransplantation. *Am J Transplant*. 2015;15(7):1748–1754.
2. Biedermann BC, Pober JS. Human vascular endothelial cells favor clonal expansion of unusual alloreactive CTL. *J Immunol*. 1999;162(12):7022–7030.
3. Dengler TJ, Pober JS. Human vascular endothelial cells stimulate memory but not naive CD8+ T cells to differentiate into CTL retaining an early activation phenotype. *J Immunol*. 2000;164(10):5146–5155.
4. Lakkis FG, Lechler RI. Origin and biology of the allogeneic response. *Cold Spring Harb Perspect Med*. 2013;3(8):a014993.
5. Abrahimi P, et al. Blocking MHC class II on human endothelium mitigates acute rejection. *JCI Insight*. 2016;1(1):e85293.
6. Merola J, et al. Progenitor-derived human endothelial cells evade alloimmunity by CRISPR/Cas9-mediated complete ablation of MHC expression. *JCI Insight*. 2019;4(20):129739.
7. Cross AR, Glotz D, Mooney N. The role of the endothelium during antibody-mediated rejection: from victim to accomplice. *Front Immunol*. 2018;9:106.
8. Zhang R. Donor-specific antibodies in kidney transplant recipients. *Clin J Am Soc Nephrol*. 2018;13(1):182–192.
9. Butler CL, Valenzuela NM, Thomas KA, Reed EF. Not all antibodies are created equal: factors that influence antibody mediated rejection. *J Immunol Res*. 2017;2017:7903471.
10. Fang C, et al. ZFYVE21 is a complement-induced Rab5 effector that activates non-canonical NF-κB via phosphoinosotide remodeling of endosomes. *Nat Commun*. 2019;10(1):2247.
11. Jane-Wit D, et al. Alloantibody and complement promote T cell-mediated cardiac allograft vasculopathy through noncanonical nuclear factor-κB signaling in endothelial cells. *Circulation*. 2013;128(23):2504–2516.
12. Xie CB, et al. Complement membrane attack complexes assemble NLRP3 inflammasomes triggering IL-1 activation of IFN-γ-primed human endothelium. *Circ Res*. 2019;124(12):1747–1759.
13. Carson WE, et al. A potential role for interleukin-15 in the regulation of human natural killer cell survival. *J Clin Invest*. 1997;99(5):937–943.
14. Zhang X, Sun S, Hwang I, Tough DF, Sprent J. Potent and selective stimulation of memory-phenotype CD8+ T cells in vivo by IL-15. *Immunity*. 1998;8(5):591–599.
15. Waldmann TA. The biology of interleukin-2 and interleukin-15: implications for cancer therapy and vaccine design. *Nat Rev Immunol*. 2006;6(8):595–601.
16. Chirifu M, et al. Crystal structure of the IL-15-IL-15Ralpha complex, a cytokine-receptor unit presented in trans. *Nat Immunol*. 2007;8(9):1001–1007.
17. Schluns KS, Klonowski KD, Lefrançois L. Transregulation of memory CD8 T-cell proliferation by IL-15Ralpha+ bone marrow-derived cells. *Blood*. 2004;103(3):988–994.
18. Dubois S, Mariner J, Waldmann TA, Tagaya Y. IL-15Ralpha recycles and presents IL-15 In trans to neighboring cells. *Immunity*. 2002;17(5):537–547.
19. Burkett PR, Koka R, Chien M, Chai S, Boone DL, Ma A. Coordinate expression and trans presentation of interleukin (IL)-15Ralpha and IL-15 supports natural killer cell and memory CD8+ T cell homeostasis. *J Exp Med*. 2004;200(7):825–834.
20. Beilin C, et al. Dendritic cell-expressed common gamma-chain recruits IL-15 for trans-presentation at the murine immunological synapse. *Wellcome Open Res*. 2018;3:84.
21. Brilot F, Strowig T, Roberts SM, Arrey F, Münz C. NK cell survival mediated through the regulatory synapse with human DCs requires IL-15Ralpha. *J Clin Invest*. 2007;117(11):3316–3329.
22. Mishra A, Sullivan L, Caligiuri MA. Molecular pathways: interleukin-15 signaling in health and in cancer. *Clin Cancer Res*. 2014;20(8):2044–2050.
23. Ring AM, et al. Mechanistic and structural insight into the functional dichotomy between IL-2 and IL-15. *Nat Immunol*. 2012;13(12):1187–1195.
24. Tagaya Y, et al. Generation of secretable and nonsecretable interleukin 15 isoforms through alternate usage of signal peptides. *Proc Natl Acad Sci USA*. 1997;94(26):14444–14449.
25. Ouyang S, Hsuchou H, Kastin AJ, Pan W. TNF stimulates nuclear export and secretion of IL-15 by acting on CRM1 and ARF6. *PLoS ONE*. 2013;8(8):e69356.
26. Oppenheimer-Marks N, Brezinschek RI, Mohamadzadeh M, Vita R, Lipsky PE. Interleukin 15 is produced by endothelial cells and increases the transendothelial migration of T cells in vitro and in the SCID mouse-human rheumatoid arthritis model in vivo. *J Clin Invest*. 1998;101(6):1261–1272.
27. Lee PH, et al. Host conditioning with IL-1β improves the antitumor function of adoptively transferred T cells. *J Exp Med*. 2019;216(11):2619–2634.
28. Pober JS, Sessa WC. Evolving functions of endothelial cells in inflammation. *Nat Rev Immunol*. 2007;7(10):803–815.
29. Savan R, Ravichandran S, Collins JR, Sakai M, Young HA. Structural conservation of interferon gamma among vertebrates. *Cytokine Growth Factor Rev*. 2009;20(2):115–124.
30. Ryffel B. Introduction. In: Richter GW, Solez K, eds. International Review of Experimental Pathology. Vol 34. Cambridge, Massachusetts, USA: Academic Press; 1993:3–6.
31. Qin L, et al. Complement C5 inhibition reduces T cell-mediated allograft vasculopathy caused by both alloantibody and ischemia reperfusion injury in humanized mice. *Am J Transplant*. 2016;16(10):2865–2876.
32. Nishimura H, Fujimoto A, Tamura N, Yajima T, Wajjwalku W, Yoshikai Y. A novel autoregulatory mechanism for transcriptional activation of the IL-15 gene by a nonsecretable isoform of IL-15 generated by alternative splicing. *FASEB J*. 2005;19(1):19–28.
33. Merola J, Jane-Wit DD, Pober JS. Recent advances in allograft vasculopathy. *Curr Opin Organ Transplant*. 2017;22(1):1–7.
34. Zhang M, et al. IL-15 enhanced antibody-dependent cellular cytotoxicity mediated by NK cells and macrophages. *Proc Natl Acad Sci USA*. 2018;115(46):E10915–E10924.
35. Hovland A, et al. The complement system and toll-like receptors as integrated players in the pathophysiology of atherosclerosis. *Atherosclerosis*. 2015;241(2):480–494.
36. Morgan BP. Complement in the pathogenesis of Alzheimer's disease. *Semin Immunopathol*. 2018;40(1):113–124.
37. Thurman JM, Yapa R. Complement therapeutics in autoimmune disease. *Front Immunol*. 2019;10:672.